ISTITUTO NAZIONALE DI FISICA NUCLEARE

Sezione di Milano

QLASA: A COMPUTER CODE FOR QUENCH SIMULATION IN ADIABATIC MULTICOIL SUPERCONDUCTING WINDINGS

Lucio Rossi [1], Massimo Sorbi [2],

[1] *Università degli Studi di Milano, Dip. di Fisica, via Celoria 16, I-20133 Milano, Italy. At present on leave at CERN, Geneva*
[2] *Università degli Studi di Milano, Dip. di Fisica e INFN Sez. di Milano, via Celoria 16, I-20133 Milano, Italy*

Abstract

Prediction of the quench evolution is an important task in designing superconducting magnets. Especially when different coils are coupled together, with possibility of energy exchange among them, very dangerous situation may happen, not easy to predict with simple analytical evaluation. The code QLASA described in this report is originated from the codes DYNQUE and QLASA in use at the superconducting magnet group of the LASA laboratory (University and INFN-Milan): it is mainly intended for adiabatic multiple solenoids, with different power supplies, but can now deal partially with different geometries. It can be used as a design tool, since it allows to control many parameters, it treats the windings as a medium of average properties (that may differ along the three dimensions) and it is coupled with an extensive custom library of cryogenic properties, although its main use has been restricted so far to NbTi and Nb3Sn conductors. It is particularly useful when internal voltages and internal temperatures need to be computed.

The report describes the winding modeling, all steps of thermal and electrical computations and how they are separated as well as the coupling with the cryogenic library. The limitations of the codes, written in F77, are explained and underlined, as well as the suggestion to use it in geometry different from the axis-symmetric. Finally a few examples of input files are given and comparisons among predictions and experiments are reported.

1.   INTRODUCTION

The aim of this work is to describe the computer code QLASA[1] written for the prediction and the study of the propagation of the quench in superconducting magnets. The code is intended in particular for magnets composed of multiple coils connected in series or powered by different supplies and inductively coupled, allowing also to describe the effect of passive inductively coupled elements (like restraining cylinders). The code was originally intended for superconducting solenoids, where the azimuthal symmetry for the magnetic field is present, but can now handle, with proper modelling, some simple 3D cases like racetrack and, to some extend, dipoles and multipoles. However use in 3-D cases may requires discussion with the authors.

The propagation of the transition is dealt in a pseudo-analytical mode (basically following the treatment of [1] but the user can easily select different models for the quench velocity or can input initial quench velocities values directly. In the last years some researchers have preferred to adopt a different approach for this kind of problem: the equation of the heat diffusion and of the current evolution are solved with F.E. code, and the velocity of the quench is given in the input data as a free parameter [2]. Other, more complete, codes, like [3], computes all parameters by solving the heat diffusion and applying a custom discretization of the topology. From our point of view an analytical approach has the vantage to allow calculating directly the quench velocity from the material properties of the magnet in a transparent and easy-to-verify way.

This code is the result of several studies of the quench propagation in superconducting coils. A previous version is the code Dynque [4] from which many parts of the code derived. During the years most of the subroutines have been changed and others have been included, in order to foresee the study of other cases like magnets working in persistent mode [5] or magnets for detectors [6].

2.   GENERAL FEATURES

The program has been developed with the following features:
➢ Capability to predicts the effects of a quench event in multiple adiabatic windings, in which several coils are wounded with cable of different materials; the coils may be connected in series or powered by different power supplies. The program deals also with coils (or passive elements) inductively coupled. The quench originates in one (or more)

---

[1] **QLASA** means : **Q**uench code developed at **LASA** laboratory; actually the code is the fruit of a long work of students of L. Rossi starting in 1990 with Gabriele Varieschi for the cryogenic properties, Stefano Piuri, Marina Canali, who wrote the first complete version, "Dynque" (whose topology and thermal calculations are still used), Massimo Sorbi, who among other improvements made the modification to treat persistent coils, Ferdinando Ametrano, who re-organised the code and the interface with the cryogenic library, Linda Imbasciati, who tested the code for dipoles and Matteo Pellegatta, who made the modifications for race track coils and introduced a special velocity computation for aluminum stabilized conductor.
Since 1999 the code is maintained by M. Sorbi (massimo.sorbi@mi.infn.it).
Here L. Rossi wants to express his sincere gratitude to the all above mentioned students that in years among 1990 and 2000 have worked, used and improved the code.

point at the initial time. Further quenches originating in other points are allowed, however quenches starting from an extended zone are not foreseen (although they can be treated with some approximations).

➢ Possibility to evaluate voltages between intermediate voltage taps each coil may be provided with. As it will be widely discussed in the following chapters, this is a very important option in order to study the quench propagation velocities in transverse direction. A very flexible structure for the positioning of voltage taps allows calculating intermediate voltage, both in the case of coils wound with solenoid technique and with the "pancake" technique.

➢ A flexible structure for the program, which allows changing or modifying the evaluation of a single quantity leaving the others unchanged so that the program might be easily improved, if it's necessary. Actually different formulations for quench propagation velocity may be used in order to compare simulation and experimental results, including the possibility of direct input, as initial data, of the longitudinal velocity. This is then scaled during the program with the current. The codes has been mainly used in adiabatic coils, impregnated, where the exchange with liquid helium is not important for the quench propagation, however its structure allows to use also in wetted coils.

➢ The coils can work in connection with a power supply, with a dump resistor and a switch for the current ("driven" mode), or without power supply, i.e. in "persistent" mode with shunt resistors.

➢ The code has been used only in LTS magnets, NbTi and Nb_3Sn, however by using suitable properties for the materials it should be able to describe HTS coils as well.

The main limitations of QLASA are:

a. Even for solenoids it does not describe properly split coils, i.e. when a considerable gap is left in the mid plane. This limitation might be removed in future, since it has to do with the way the magnetic field of multiple coils is calculated (assuming that each outer solenoids is longer than each inner one, allowing a simple approximation);

b. The description of the unit cell is very suited to rectangular conductor; if the conductor cross section is circular, the codes computes the equivalent rectangular cell, see input description.

c. The coil is a sort of continuous medium for the quench propagation and thermal and electric properties are averaged. For this reason the code is less suitable for magnets wounds with one or two layers (or turns) with big cable. It certainly fits better coils whose radial and height size are much larger than the cable size, i.e. many turns and many layers are involved.

d. The code has no thermal connection among coils. Each one is a boundary for quench propagation. However with some effort and artifice this limitation can be overcome.

e. Conductor dominated by magnetic diffusion (i.e. with large matrix of very high conductivity) should be dealt with care and results are very much dependent on the

applicability of a particular model developed and tested for the coils of ATLAS detector toroids.

f. AC losses and magnetization effects are not take in to account (although they might partially be treated as they can be somehow accounted in the effective resistivity of some components).

g. The integration time step is constant during all a run: consequently, if some parameters like current or temperature changes fast in a phase of the simulation, a short time step is required for all the run, with the inconvenience of long output files and long calculation time

h. Very high value of the dump resistors might affect the stability of the electric circuit solver. This problem can be cured by refining the time integration step.

In this chapter the flow-chart of the program is discussed, leaving to the following chapters a detailed discussion about the structure of each subroutine, on how the different quantities are worked out and about what approximations have been used. In order to gain in flexibility, the computer program is conceived like a collection of subroutines, each one having a particular target or calculating a particular quantity, linked together by the main program. Fig.1 shows the *Qlasa* flow-chart.

The input data are read by the subroutine SUBREAD and they are:

➢ Title of the run and type of problem ("driven" mode or "persistent" mode).
➢ Number of temporal steps and time increment to be used.
➢ Number and geometric dimensions of the windings.
➢ Number and position of the voltage taps.
➢ Time and position of the quench starting point.
➢ Operating current, critical current of the cable and magnet field locations that will be later specified.
➢ Self and mutual inductances.
➢ Cable components and their percentage in the unit cell.
➢ Information about electric circuit: dumping resistance, delay time, arc time, maximum voltage of the power supply, number of magnet electrically connected in series and independently supplied.
➢ Information about the liquid helium bath for the evaluation of the time of evaporation of all the liquid.

The detailed instructions for the input file are reported in the section 4.

After the input data reading, in the subroutine SUBCOST some constants necessary to the run are calculated; subsequently the files are opened by the subroutine SUBOPEN, the subroutine MPZ calculates the minimum propagating zones and the minimum propagating energies and the subroutine SUBWRITE-1 heads the files. At this point the first temporal loop starts. At first the current I(t) and the magnetic field on each winding are calculated. Then, if a coil is quenched, the quench propagating velocities in longitudinal, axial and radial directions are evaluated by SUBSPEED. The calculation of these velocities depends on the

values of the average thermal conductivities in the different direction computed in the subroutine THK. After that, the dimension of the 3-D ellipsoid axes, which represent the normal zone volume, are updated; by means of these ellipsoid axes, the subroutine SUBVOL evaluates the volume of the resistive zone inside each section, which are delimitated by adjacent voltage taps in the radial and axial direction. The knowledge of the normal zone volume and the average value of the resistivity at the actual temperature and field, calculated by the subroutine RHO, makes possible to obtain the resistance of each section and the total resistance of the magnets. The temperature of the normal zone is then computed by solving the heat balance equation and using the subroutines CP and CPMET to have the average specific heat. THK, RHO, CP and CPMET are all linked to the files containing the properties of the different materials in a range of temperature from 2 K to 300 K.
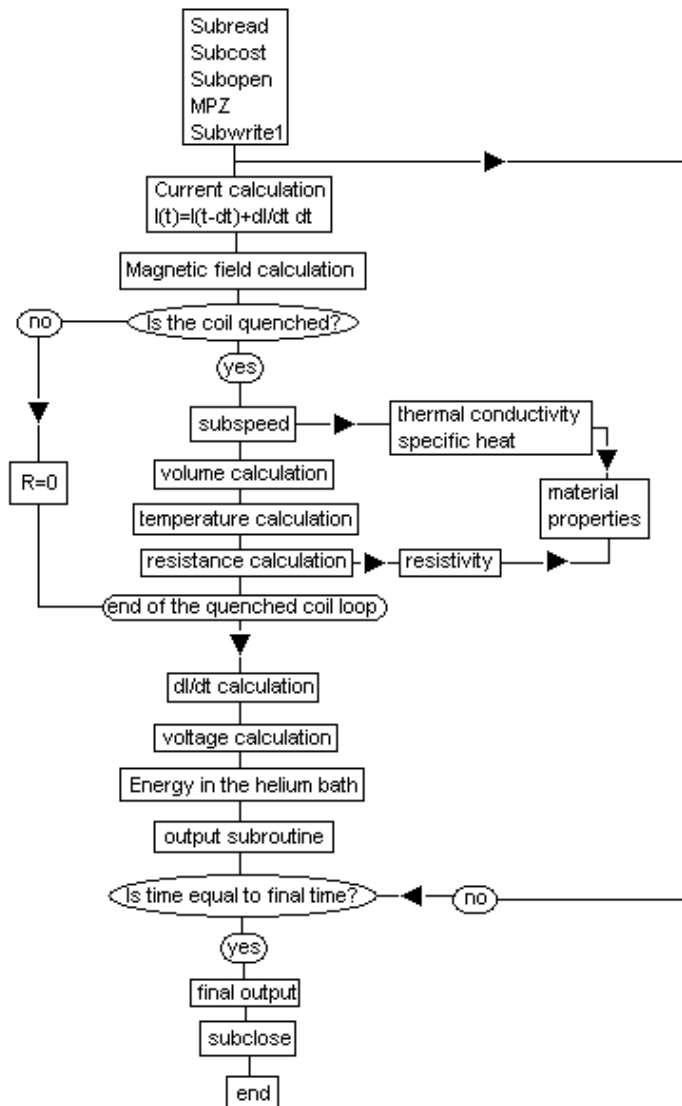

FIG. 1: Flow-chart of the computer code Qlasa.

If a coil is not quenched, all these steps are skipped, the normal zone volume as well as the magnet resistance is set equal to zero, while the temperature inside the winding is set equal to the bath temperature.

When these quantities are obtained for each magnet, the subroutine DCURR solves the electric circuit equations providing the values for the ratio dI/dt for each magnet. Then the voltage at each voltage step in each coil is calculated as well as the energy dissipated in the winding during the temporal steps for the evaluation of the helium evaporation.

There are several output files providing the values obtained for different quantities; some of them are automatically generated by the program and written by the subroutine SUBWRITE2. For the generic n-th coil they are:

➢ **Q*n*.out** which contains for each time step the values of time, current, hot spot temperature, resistive volume increment and total voltage across the winding.
➢ **Vel*n*.out** which reports the longitudinal and transversal quench propagation velocities that are necessary for resistive volume evaluation (cfr. 3.2)
➢ **Curr*n*.out** which reports the current in the magnet, the current flowing in the dumping resistor, the current delivered by the power supply and the value of dI/dt for each temporal step.

Moreover the user can choose to have some additional information by setting in input the parameter *iout=1*. In this case these additional files are generated:

➢ **Qa*n*.out** which reports the voltage across each section the coil is subdivided by voltage taps. The values are reported in the following order: first axial subdivision, from the internal radial zone to the external radial zone; second axial subdivision, from the internal radial zone to the external radial zone; etc. etc.
➢ **Field*n*.out** which contains the magnetic field that is necessary for quench propagation velocity calculation (cfr. 3.4).
➢ **Thcond*n*.out** which contains the values of the thermal conductivity in longitudinal, radial and axial directions in the locations where the propagation velocities are required.
➢ **Volum*n*.out** containing the normal zone volume and its dimensions in the coils at each temporal step. The values are reported in the following order: first axial subdivision, from the internal radial zone to the external radial zone; second axial subdivision, from the internal radial zone to the external radial zone; etc. etc.
➢ **Res*n*.out** containing the resistance of each section of the coils at each temporal step. The values are reported in the following order: first axial subdivision, from the internal radial zone to the external radial zone; second axial subdivision, from the internal radial zone to the external radial zone; etc. etc.
➢

When all the temporal steps have been executed, the subroutine SUBWRITE-3 writes in the main output file some information about the state of the coil system at the end of quench evolution like the total energy dissipated in the magnet and the maximum voltage and temperature values.

3. THE CODE QLASA: DETAILED DISCUSSION

3.1 Longitudinal propagation velocity

In order to describe how the normal zone spreads up in a magnet we need to discuss its propagation velocity and, as a coil is a strongly anisotropic medium, different directions are to be taken in account. Let's first consider a single wire: as regards the velocity in longitudinal direction (i.e. parallel to the cable) the normal-superconducting boundaries are usually described by a plane thermal wave travelling velocity v_l. The analytical expression for v_l depends by the model adopted in the analysis, and it can be selected by the user as described in the following items. In order to fit the experimental data, it could be necessary to increase or decrease the calculated value of v_l. For this reason the user can multiply this value for a coefficient given in the input file (*corvz*).

3.1.1 First model

An analytical expression for v_l, valid for adiabatic coils, can be obtained by selecting *kvl*=0 in the input file. This situation can be applied for superconducting magnet with superconductor stabilized with copper or aluminium, if the diffusion time of the current in the stabilizing metal is negligible. The expression is obtained by solving the heat balance equation in the one-dimensional case, neglecting the thermal exchange in transversal direction [1],[7],[8].

$$\begin{cases} v_l = \dfrac{J}{\gamma C_{av.met}} \sqrt{\dfrac{L\Theta_m}{\Theta_m - \Theta_0}} \\ \Theta_m = \dfrac{\Theta_g + \Theta_c}{2} \end{cases} \tag{1}$$

Θ_0 is the operation temperature of the magnet, J the current density (averaged over the unit cell), $\gamma C_{av.met.}$ the volumetric specific heat averaged over the metallic part of the unit cell (see section 3.5.2), L the Lorenz number, Θ_c is the critical temperature at J=0 and Θ_g is the temperature at which ohmic heat generation starts (critical generation temperature) (see section 3.3)

3.1.2 Second model

This model, which can be chosen selecting *kvel*=1, is similar to the first model but without considering the Wiedmann-Franz law for the product of the electrical resistivity and the thermal conductivity:

$$\begin{cases} v_l = \dfrac{J}{\gamma C_{av.met}} \sqrt{\dfrac{\rho_{av.} \cdot k_l}{\Theta_m - \Theta_0}} \\ \Theta_m = \dfrac{\Theta_g + \Theta_c}{2} \end{cases} \tag{2}$$

In this case $\rho_{av.}$ and k_l represent respectively the electrical resistivity and the longitudinal thermal conductivity averaged over the unit cell (see paragraph 3.5.3 and 3.5.1)

3.1.3 Third model.

This model can be applied in the case the current diffusion time in the stabilizing metal is not negligible (*kvel*=2). This is the typical case when the matrix has a very low resistance and considerable size: because of this the current does not distribute uniformly in a negligible time (with respect to longitudinal diffusion time) in the whole cross section. Then the $J_{stabilizer}$ is locally much higher than in a uniform case, causing the release of an energy density surplus in the cable due to Joule effect; this surplus is much larger than the value that there would be with uniform distribution of current (reached asymptotically). Since the thermal diffusion is the same or even enhanced, with respect to standard stabilizer, in case of high conductivity matrix, one of the important consequences of such an energy release is the increase of the longitudinal quench propagation velocity [6]. This situation occurs, for example, in superconducting magnets used for large HEP detectors, having a large quantity of stabilizing metal with RRR>400 (normally pure aluminum) surrounding the Rutherford cable that is composed by the superconductor and copper. For this reason the code can foresees the presence of aluminum in the stabilizing metal and copper in the inner cable or wire. The expression for the longitudinal velocity v_l is then:

$$\begin{cases} v_l = \dfrac{I}{\gamma C_{av.met.}\sqrt{(A-A_0)\cdot a}} \sqrt{\dfrac{\rho_{eff}k_{Al}}{\Theta_m - \Theta_0}} \\ \Theta_m = \dfrac{\Theta_g + \Theta_c}{2} \end{cases} \tag{3}$$

where all symbols have the same meaning of expression (1), *I* is the current in the magnet, *A* is the unit cell area (*uca* in the input file), A_0 is the area of the Rutherford cable (*acu* in the input file), *a* is a free parameter which represents the diffusion area (*adif* in the input file) k_{Al} is the thermal conductivity of aluminum and ρ_{eff} is the effective resistivity given by the parallel of the resistance of the copper and aluminum, i.e.:

$$\rho_{eff} = \frac{a\rho_{Cu} \cdot \rho_{Al}}{A_0 \rho_{Al} + (a - A_0)\rho_{Cu}}$$

k_{Al} and ρ_{eff} are internally calculated by the code at each temporal step.

In the ATLAS conductor, typical values of *a* are 60-90 mm², for quench velocity ranging between 5 m/s and 20 m/s (see pag. 55 of [6])

3.1.4 Fourth model

If *kvl*=3 the model is again applied for conductor with large quantity of stabilizing metal and so with large current diffusion time; in this case the model utilized by the code to get the longitudinal propagation velocity is expressed by the following equation [6]:

$$v_l = \left[\frac{I^2 \cdot \rho_{Cu} \cdot k_{Al}}{\gamma^2 C_{av.met.}^2 A_0 (A - A_0) \cdot (\Theta_m - \Theta_0)} - \frac{(A - A_0) \cdot \rho_{Cu} \cdot k_{Al}}{\gamma C_{av.met.} \tau_c A_0 \rho_{Al}} \right]^{1/2} \quad (4)$$

In this block a new variable has to be calculated: it is the current characteristic diffusion time τ_c, which expression is:

$$\tau_c = \frac{l^2 \cdot \mu_0}{\pi^2 \cdot \rho_{Al}} \quad (5)$$

l is the characteristic diffusion length, inserted in the input file (with the name *difle*) and estimated by the conductor size.

Since the expression (4) arises from a Taylor development, there are values of magnet current where the argument of the square root becomes negative and the expression loses its physical meaning. For this reason in this block a variable control has been inserted: if the argument of the square root is negative the longitudinal quench propagation velocity is calculated in the traditional way with eq. (1); as consequence the key *kvl* in changed in to *kvl*=0 from the temporal step after the one in which it is recognized that the square root is negative. This control allows the program to calculate the quench longitudinal propagation velocity for every value of magnet current. It is however to remark that around the value that makes negative the argument of the square root, where the velocity calculation method changes, the result obtained by the traditional model (*kvl*=0) can underestimate the real value. This because it does not consider the magnetic diffusion effect. At lower current where the traditional method works, and at high current where the square root does not become negative the result from the two models are more realistic.

3.1.5 Fifth model

If *kvl*=4 the way in which the code calculates the longitudinal propagation velocity is specific for rectangular conductor, where the magnetic diffusion can be considered in two dimensions [6]. The method is very similar to the case *kvl*=3, but the diffusion area has a more detailed mathematical expression that puts in evidence the two different dimensions. The expression is:

$$v_l = \left[\frac{I^2 \cdot \rho_{Cu} \cdot k_{Al}}{\gamma^2 C_{av.met.}^2 A_0 (A - A_0) \cdot (\Theta_m - \Theta_0)} - \frac{(\alpha \cdot d - A_0) \cdot \rho_{Cu} \cdot k_{Al}}{\gamma C_{av.met.} \tau_x A_0 \rho_{Al}} - \frac{(\beta \cdot c - A_0) \cdot \rho_{Cu} \cdot k_{Al}}{\gamma C_{av.met.} \tau_y A_0 \rho_{Al}} \right]^{1/2} \quad (6)$$

Also in this block the two characteristic diffusion times are the new variables τ_x and τ_y. The expression is the same as (5), but the direction of the two characteristic diffusion lengths are specified. Moreover these lengths are calculated starting from the dimensions of the cable, so that the resulting diffusion times are as follows:

$$\tau_x = \frac{l_x^2 \cdot \mu_0}{\pi^2 \cdot \rho_{Al}} = \frac{(\alpha - c)^2 \cdot \mu_0}{4\pi^2 \cdot \rho_{Al}} \tag{7}$$

$$\tau_y = \frac{l_y^2 \cdot \mu_0}{\pi^2 \cdot \rho_{Al}} = \frac{(\beta - d)^2 \cdot \mu_0}{4\pi^2 \cdot \rho_{Al}} \tag{8}$$

where α and β are the two dimensions of the rectangular aluminum stabilizing cross section, c and d the two dimensions of the Rutherford cable. The variables are respectively called in the code *stabl* (stabilizer length), *sst* (short stabilized), *lrtf* (long Rutherford) and *srt* (short Rutherford).

The consideration about the weak point of the model due to the approximation in the Taylor development when *kvl*=3 is to be remarked also in this case. The adopted solution is the same: when the argument of the square root is negative, the longitudinal propagation velocity is calculated with (1) and *kvl* is changed in to *kvl*=0 for all the following temporal steps.

3.1.6 Presence of large heater

In order to simulate the increase of temperature of the wave front due to the presence of a large heater, in all the models, the operating temperature, which is reported in eq. (1), (2), (3), (4) and (6), can be increased by a quantity controlled by the input parameter *tedi*. Normally its value is set equal to zero.

3.2   Transversal propagation velocity

For the transversal propagation velocity, let's consider a solenoidal winding: the heat produced by ohmic dissipation will diffuse through the insulation in transverse direction too, i.e. perpendicularly to the cable itself. For the quench propagation velocity in the transverse direction, the following expression has been adopted, as suggested by Wilson [1]:

$$v_t = v_l \cdot \frac{(\gamma C)_{av.met}}{(\gamma C)_{av.}} \cdot \sqrt{\frac{k_t}{k_l}} \tag{9}$$

where $(\gamma C)_{av.}$ is the specific volumetric heat averaged over the total cross section, while $(\gamma C)_{av.met}$ is averaged over the metallic part only.

Due to the fact that k_t is generally different if evaluated in radial direction (i.e. along the coil radius) or in the axial direction (i.e. parallel to the coil axis), the radial and axial quench propagation velocities v_r and v_a will be different too. Moreover, because the term in expression (9) are sensible to the magnetic field value, which could be different from a zone of the magnet respect others, v_r and v_a have been splitted in two values ("in" and "out" for v_r and "up" and "down" for v_a), in order to take in consideration different transversal propagation velocities for the four transversal propagation wave fronts of the transition zone.

Also in this case the user can multiply the transversal velocities for some correction coefficients in order to better fit the calculated value with the experimental value. The name of this correction coefficient in the input file is: *corvri* and *corvre* for the internal and external radial velocities; *corvhu* and *corvhd* for the "up" and "down" axial velocities.

3.2.2 Important note for longitudinal velocity dominant respect transversal velocities.

The code is specifically optimized for large magnets, where the transversal velocities are dominant respect the longitudinal velocity for the propagation of the quench from one turn to the others. During the run, at each temporal step, a check is done in order to verify whether this condition is fulfilled for the axial direction. An alarm notice is written in the main output file when this condition is not fulfilled: in this case all the results must be double checked carefully because the volume of the normal zone is not anymore a simple ellipsoid as it is assumed in the subroutine for volume calculation.

3.3   Critical temperature $\Theta_c(B)$ and heat generation (current sharing) temperature $\Theta_g(B,J)$

The critical temperature $\Theta_c(B)$ and the generation temperature $\Theta_g(B,J)$ are used for the evaluation of the quench propagation velocity as described in paragraph 3.1 and to evaluate the presence of spontaneous new quenches in the magnet. This heat generation temperature is also called Current Sharing Temperature.

The program foresees two options: if the input parameter *isc*=0, the value for the critical temperature $\Theta_c(B)$ at the current density J=0 and field B is given by the empirical formula of Lubell [9]:

$$\Theta_c(B,0) = \Theta_{c0}\left(1 - \frac{B}{B_0}\right)^x \tag{10}$$

where the parameters Θ_{c0}, B_0 and x are given in the input file with the names *themax, bmax* and *xlub* respectively.

The generation temperature $\Theta_g(B,J)$ at the current density J and field B scales linearly with the current and is given by:

$$\Theta_g(B,J) = \Theta_c(B,0) - \left[\Theta_c(B,0) - \Theta_{cc}\right]\frac{J}{J_{c0}(B)} \tag{11}$$

where $J_{c0}(B)$ is the critical current density at the temperature $\Theta = \Theta_{cc}$ and magnetic field B. A non-linear relationship between $J_{c0}(B)$ and B is assumed at the temperature Θ_{cc}:

$$J_{c0}{}^\alpha B^\beta = m \cdot B + q \tag{12}$$

The value of Θ_{cc}, α and β are given in the input file (the parameter *thecc, alfa, beta* respectively), whereas the value for *m* and *q* are obtained by interpolation from $n \geq 2$

experimental couples of J_{cn} and B_n. The parameters n, J_{cn} and B_n are given in the input file with the name *num(Ic-B), Ic* and *B*.

Typical values for Θ_{c0}, B_0, x, α and β are the following:

	Θ_{c0} (K)	B_0 (T)	x	α	β
NbTi	9.2	14.5	0.59	1	0
Nb$_3$Sn	18.3	22.0	0.55	0.5	0.25

If the input parameter *isc=1*, the value for the critical temperature $\Theta_c(B)$ and generation temperature $\Theta_g(B,J)$ are calculated according the Summers's empirical formula [10], which are valid for Nb$_3$Sn. In the code $\Theta_c(B)$ and $\Theta_g(B,J)$ are respectively obtained by numerically reverting the following equations:

$$B_{c2}(\Theta) = B_{c20}\left[1-\left(\frac{\Theta}{\Theta_{c0}}\right)^2\right]\cdot\left\{1-0.31\cdot\left(\frac{\Theta}{\Theta_{c0}}\right)^2\cdot\left[1-1.77\cdot\ln\left(\frac{\Theta}{\Theta_{c0}}\right)\right]\right\} \tag{13}$$

and

$$J_c(B,\Theta) = C\left[1-\left(\frac{\Theta}{\Theta_{c0}}\right)^2\right]^2\cdot\left[1-\frac{B}{B_{c2}(\Theta)}\right]^2\cdot B^{-1/2} \tag{14}$$

where the constant B_{c20} and C are calculated in the subroutine SUBCOST and assume the following values:

$$B_{c20} = -\frac{q}{m}\left[1-\left(\frac{\Theta_{cc}}{\Theta_{c0}}\right)^2\right]^{-1}\cdot\left\{1-0.31\cdot\left(\frac{\Theta_{cc}}{\Theta_{c0}}\right)^2\cdot\left[1-1.77\cdot\ln\left(\frac{\Theta_{cc}}{\Theta_{c0}}\right)\right]\right\}^{-1} \tag{15}$$

$$C = J_{c0}(B)\cdot\left[1-\left(\frac{\Theta_{cc}}{\Theta_{c0}}\right)^2\right]^{-2}\cdot\left[1-\frac{B}{-\dfrac{q}{m}}\right]^{-2}\cdot B^{1/2}\Bigg|_{B=5T} \tag{16}$$

3.4 Magnetic field

In order to evaluate the quench propagation velocity, it is necessary to know the magnetic field inside each coil, since Θ_m, $\rho_{av.}$, k_l and k_t depends on field. In order to obtain a field map for every winding at each temporal step we use the following approach. Let's consider N concentric solenoids in cylindrical coordinate system r, ϕ, z with the z axis with the coil axis and the plane $z=0$ coincident with the symmetry plane of each winding: the

magnetic field $Btot_k$ at radius r and height z of the k-th solenoid will be given for any angle by:

$$Btot_k = B_k(r,z,I_k) + \sum_{i=k+1}^{N} B_{0i}(I_i) + Bext_k \tag{16}$$

where:

$B_k(r,z,I_k)$ is the self field generated by the k-th coil at the request point P(r,z) at the current I_k ;

$B_{0i}(I_i)$ is the magnetic field produced by the i-th winding inside its bore at the current I_i ;

$Bext_k$ is the external field of the k-th coil.

In relation (16) the windings are to be considered numbered from the inner one to the outer one (a must for the correct use of the code); so in the right-end side the second term represents the contribution to the field from the magnets outside the k-th one. The basic assumption of (16) is to neglect the stray field of every (solenoidal) coil and consider the field generated inside the bore as uniform. Of course both these assumptions leads to a drastic approximation. However, very often in multiple solenoids a coil inserted in a bigger one is considerable shorter, such that the field generated by the external coil onto the internal one does not vary very much (at least at the level of accuracy requested for the material properties). Regarding this approximation it should be noticed that it may be very important, and inconvenient, for solenoid provided with important shim coils that are placed outside and do not cover the whole length of the inner coil (like the main outer shim coils in some NMR magnet design). In such a case, the user must do some kind of evaluation of the possible error.

The following values are required for each magnet by the code as input for the magnetic field evaluation:

B_{0i} that is the magnetic field produced by the i-th coil in its bore at the initial current I_{0i} (*B0i* in the input file);

$Br\mathrm{int}_i$ that is the magnetic field produced by the i-th coil at P(Rin_i, $\dfrac{H_i}{2}$) at the initial current I_{0i} (*Brinti* in the input file);

$Bh\mathrm{int}_i$ that is the magnetic field produced by the i-th coil at P($Rin_{i,}$,0) at the initial current I_{0i} (*Bhinti* in the input file);

$Brext_i$ that is the magnetic field produced by the i-th coil at P($Rout_i$, $\dfrac{H_i}{2}$) at the initial current I_{0i} (*Brexti* in the input file);

$Bhext_i$ that is the magnetic field produced by the i-th coil at P($Rout_{i,}$,0) at the initial current I_{0i} (*Bhexti* in the input file);

$Bext_i$ that is the external magnetic field in the i-th coil not due to the other windings considered in the input file (*Bexti* in the input file).

At any time the magnetic field in each request point of the *k*-th coil is obtained assuming:

➢ A linear dependence of the magnetic field $Br\,\text{int}_i$, $Bh\,\text{int}_i$, $Brext_i$, $Bhext_i$ respect the current. This means that values for the field B at the initial time are scaled with current at each temporal step;

➢ The self field of the coil *i*-th at the point P(*r,z*) is calculated by a linear interpolation of the quantities $Br\,\text{int}_i$, $Bh\,\text{int}_i$, $Brext_i$, $Bhext_i$, assuming that the field is symmetric respect the median plane of the coil $z=\dfrac{H_i}{2}$.

If a quench starts from the point P(*Rq,Zq*) at time *t*=0 inside the *k*-th coil, the normal zone spreads out during the first temporal step with velocities:

$$v_l = v_l\big[B(Rq,Zq)\big] = v_l(Rq,Zq) \tag{17}$$

$$v_r = v_l(Rq,Zq) \cdot \sqrt{\frac{k_r(Rq,Zq)}{k_l(Rq,Zq)}} \tag{18}$$

$$v_a = v_l(Rq,Zq) \cdot \sqrt{\frac{k_a(Rq,Zq)}{k_l(Rq,Zq)}} \tag{19}$$

Referring to Fig. 2, the field is to be evaluated not only in P but also in:

$A = (r_a, Zq)$
$B = (r_b, Zq)$
$C = (Rq, z_c)$
$D = (Rq, z_d)$

and the normal zone will propagate in radial and axial direction not longer symmetrically just because of different values of the magnetic field in different points. In fact in A, for example, it is:

$$v_{l(A)} = v_l\big[B(r_a,Zq)\big] \tag{20}$$

$$v_{r(A)} = v_{l(A)}(Rq,Zq) \cdot \sqrt{\frac{k_r(r_a,Zq)}{k_l(r_a,Zq)}} \tag{21}$$

$$v_{a(A)} = v_{l(A)}(Rq,Zq) \cdot \sqrt{\frac{k_a(r_a,Zq)}{k_l(r_a,Zq)}} \tag{22}$$

while the corresponding values for the quench propagation in B are certainly different because the magnetic field in B is less than in A.
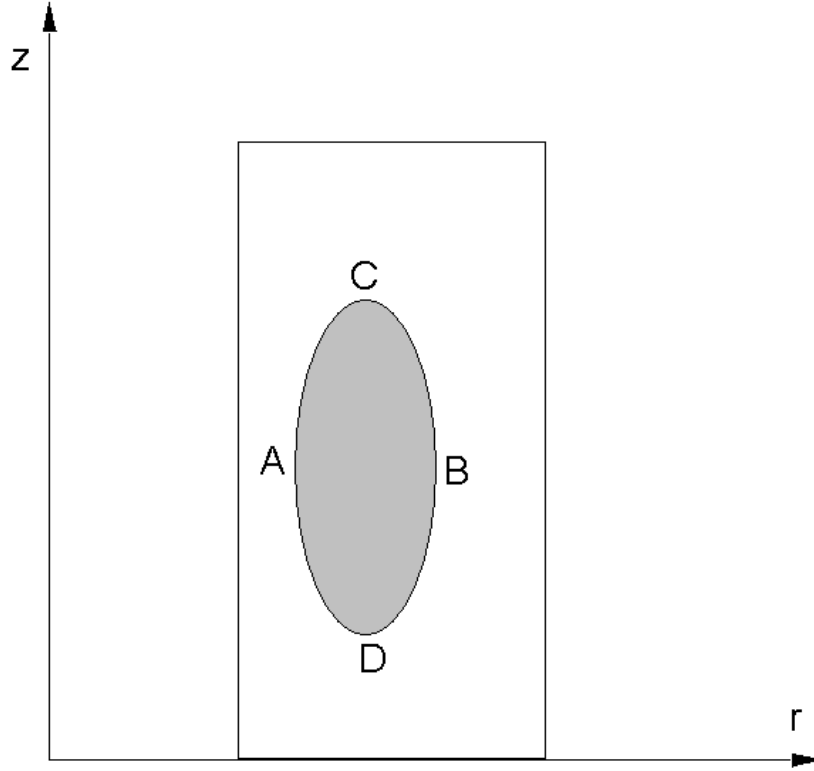
FIG. 2: Normal zone cross section

In the program the coordinates of A, B, C, D are evaluated at each temporal step being for the *n*-th:

$$r_A = Rq - \sum_{i=0}^{n} v_{r(A)}(t_i) \cdot dt$$

$$r_B = Rq + \sum_{i=0}^{n} v_{r(B)}(t_i) \cdot dt$$

$$z_C = Rq + \sum_{i=0}^{n} v_{z(C)}(t_i) \cdot dt$$

$$z_D = Rq - \sum_{i=0}^{n} v_{z(D)}(t_i) \cdot dt$$

The magnetic field is then evaluated according to the actual current flowing in each coil, and the values for v_l, v_r and v_a are obtained.

3.5 Material properties

In (1), (2), (3), (4), (6) and (9) the specific heat, thermal conductivity and resistivity must be averaged over the different constituents of the winding. For this reason the dimensions of the unit cell and the percentage of the materials are required as input data by the program. The unit cell (*uca* in the input file) is assumed to be rectangular shaped, with a

metallic core equivalent to the bare cable surrounded by a uniform layer of insulation (*alins* in the input file). The thickness of the insulation includes both the cable covering (usually glass or varnish) and the resin used for the impregnation. The area of the unit cell and the fraction of the different components must be calculated by considering a cross section of the solenoid <u>perpendicular</u> to the winding sense of the conductor.

The dependency of the physical properties with the temperature and the magnetic field is internally calculated by the subroutine XMATPRO, which collects the material properties of several elements and compounds.

3.5.1 Thermal conductivity

Regards the transverse and longitudinal thermal conductivity, they can be evaluated considering all the *Nc* components of the unit cell like thermal conductance in series or in parallel respectively. Concerning the longitudinal direction we'll have:

$$C_l = \sum_{i=1}^{Nc} C_i \tag{23}$$

C_l : effective thermal conductance in longitudinal direction.
C_i : *i*-th material's thermal conductance.

The formula (23) can be re-written as:

$$\frac{k_l \cdot S}{L} = \sum_{i=1}^{Nc} \frac{k_i \cdot S_i}{L} \tag{24}$$

from which:

$$k_l = \sum_{i=1}^{Nc} \left(k_i \cdot \frac{S_i}{S} \right)$$

$$k_l = \sum_{i=1}^{Nc} k_i \cdot f_i \tag{25}$$

Being f_i the fraction in volume, i.e. in cross section, of the *i*-th component in the unitary cell cross section (*frac* in the input file).

As far as the transverse direction, let's first consider the radial one. The unit cell is conceived like three thermal conductances in parallel to each other: the upper and the lower in Fig. 3a are made of insulating material while the central one includes both the metallic core and the insulation on the planes parallel to r=constant.
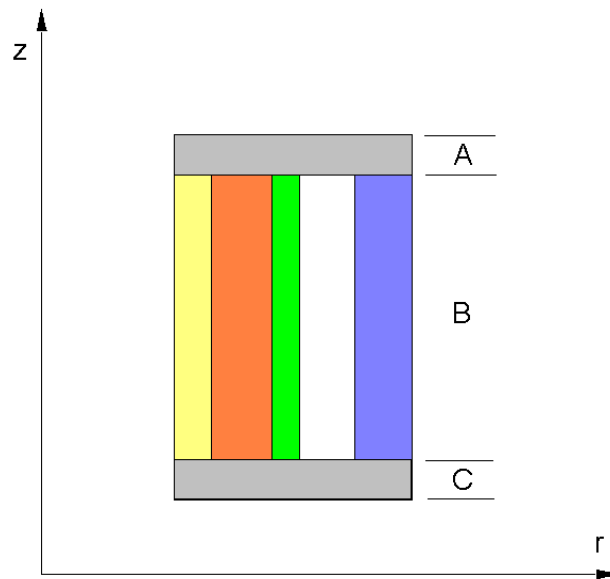
a)
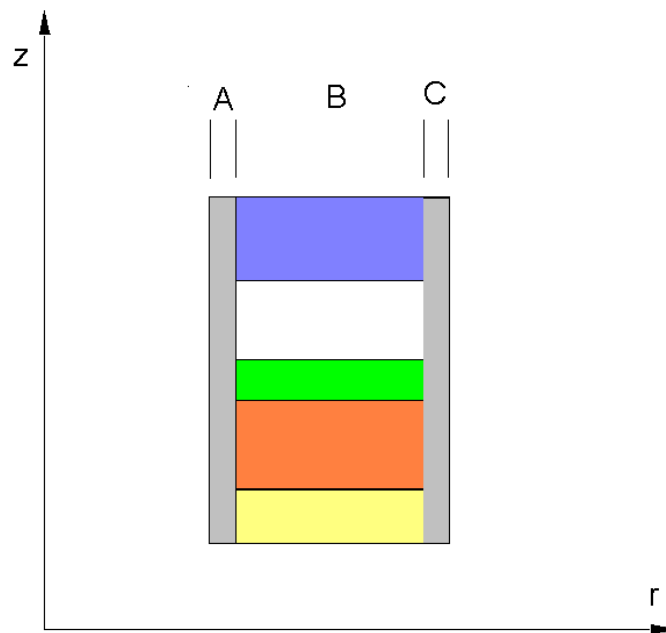
b)

FIG. 3: Unit cell model for thermal conductivity evaluation in radial (a) and axial (b) direction

The thermal conductivity in the middle layer is evaluated by assuming this section composed by layers of different materials each one having a surface $S_i = p_i \cdot S$ and being, from the thermal point of view, conductance in series to each other.

So the average thermal conductivity in B is calculated from:

$$\frac{1}{C_B} = \sum_{i=1}^{Nc} \frac{1}{C_i} \tag{26}$$

which can be re-written as:

$$k_B = \frac{L}{\sum \dfrac{L_i}{k_i}} = \frac{1}{\sum \dfrac{f'_i}{k_i}} \tag{27}$$

where f'_i is the fraction of the material inside the zone B (see Fig. 3a).
Finally k_r is obtained from:

$$k_r = k_A f_A + k_B f_B + k_C f_C$$

In the same way the thermal conductivity is evaluated in the axial direction, modeling the unit cell as it is sketched in Fig. 3b.

It's worth remarking that, because of the complex structure of the cables and insulation, a coil is a highly inhomogeneous and anisotropic medium; for this reason a right value for k_l and mainly for k_t is very hard to reach and their evaluation may be a weak point in the program. In any case this approach is certainly more suited to cases where many turn and many layers are wound, such as the discontinuity in heat transmission is averaged in multiple steps. Furthermore is clear that it is difficult in this treatment to take in account the presence of a coolant (although one can play with an effective thermal conductivity to simulate the time lag given by the coolant)

3.5.2 Specific heat

Along the longitudinal direction the heat will propagate mainly through the metallic components, since the insulation of the cable is thermally in parallel and its thermal diffusivity is orders of magnitude less than the conductor itself, while regarding transverse direction, the heat is forced to propagate also through the insulation in transverse direction. This is why in (1), (2), (4), (6) $(\gamma C)_{av.met.}$ is used instead of $(\gamma C)_{av.}$.

The temperature dependency can be calculated in two ways as following:

If the input parameter *ivel*=1, the volumetric specific heat is supposed to vary with the cube of temperature and is evaluated at the temperature $\Theta = \Theta_m$, whose value depends on current and field; for this reason it is to be calculated at each temporal step, i.e.:

$$\gamma C_{av.met.} = (\gamma C)_0 \Theta_m^{\,3}$$

where the quantity $(\gamma C)_0$ is calculated at the first step and is equal to:

$$(\gamma C)_0 = \frac{\gamma C_{av.met.}(\Theta_0)}{\Theta_0^3}$$

If *ivel*=2 the average of the specific heat is evaluated in the temperature range $\Theta_0 \leq \Theta \leq \Theta_c$, i.e.:

$$\gamma C_{av.met.} = \frac{\int_{\Theta_0}^{\Theta_c} (\gamma C(\Theta))_{av.met} \, d\Theta}{\Theta_c - \Theta_0}$$

This integral is calculated by considering the only metallic part of the components of the conductor, and it is re-calculated at each temporal step, because the value of Θ_c changes continuously.

3.5.3 Electrical resistivity

The average resistivity per unit volume is computed by assuming the different materials like electrical resistances in parallel each to the other. What is called average is actually the effective resistivity in the longitudinal direction (the current direction). In this way we'll have:

$$\frac{1}{\rho_{av}(B,\Theta)} = \sum_{i=1}^{Nc} \frac{f_i}{\rho_i(B,\Theta)}(\cos\beta)^2$$

and then

$$\rho_{av}(B,\Theta) = \left[\sum_{i=1}^{Nc} \frac{f_i}{\rho_i(B,\Theta)} \right]^{-1} \cdot \frac{1}{(\cos\beta)^2} \tag{28}$$

where $\rho_i(B_{av},\Theta)$ and f_i are respectively the resistivity and the fraction of the *i*-th component and *Nc* is the number of components of the unit cell. The term $(\cos\beta)^2$ takes in account the higher length and the lower cross section of the cable due to an eventual pitch angle for Rutherford cable. The parameter *Nc*, f_i and $\cos\beta$ are given in the input file (*nc, frac, cosbeta* respectively) whereas $\rho_i(B,\Theta)$ are calculated from the internal library of materials.

By this treatment the actual dissipation in the whole conductor is computed and not only the main stabilizer. The dissipation in the superconductor is considered by assuming it in the normal state with its own resistivity. However dissipation in the superconductor part of the conductor at the temperature below $\Theta_g(B,J)$ is not taken into account, neglecting the smooth increase of voltage near *Ic*.

3.6 Normal zone volume

Because of the strong anisotropy of the winding, it's very difficult to predict the real shape of the resistive zone at any time. The resistive zone on a section at a fixed angle is in fact quite irregularly shaped, the quench spreading faster where the magnetic field is higher, and slower in those directions where there is a high percentage of insulation or where the magnetic field is weak.

In order to be able to calculate the normal zone volume, a simplified model has been taken into account. Let's first consider the magnetic field be uniform inside the winding: the quench would spread out with velocity v_r towards the coil inner and outer radius and with velocity v_a towards the top and the bottom of the coil. In this case we assume that the normal zone envelope at any time t is the surface:

$$
\begin{cases}
\dfrac{(r-\rho_0)^2}{[R_0(t)]^2} + \dfrac{(z-\beta)^2}{[Z_0(t)]^2} + \dfrac{\Phi^2}{[\Phi_0(t)]^2} = 1 \\
R_{in} \le r \le R_{out} \\
0 \le z \le H_m
\end{cases}
\tag{29}
$$

where r, z, Φ are the radial, axial and angular coordinates in a cylindrical coordinate system; $P=P(\rho_0, 0, \beta)$ is the quench origin;

$$R_0(t) = \sum_{k=0}^{I} v_r(k) \cdot dt$$

$$Z_0(t) = \sum_{k=0}^{I} v_a(k) \cdot dt$$

$$\Phi_0(t) = \sum_{k=0}^{I} \frac{v_l(k)}{\rho_0} \cdot dt$$

I=actual temporal step, k=index of temporal steps.

The surface (29) satisfies the following conditions:

- At fixed radius r the (29) is an ellipse (Fig. 4.a) in the angular and axial coordinates with centre $O_1(0,\beta)$ and semi-axes:

$$
\begin{cases}
\phi(r,t) = \phi_0(t)\alpha(r,t) \\
Z(r,t) = Z_0(t)\alpha(r,t) \\
[\alpha(r,t)]^2 = 1 - \dfrac{(r-\rho_0)^2}{[R_0(t)]^2}
\end{cases}
$$

- At fixed angle ϕ the (29) is an ellipse (Fig. 4.b) in the radial and axial coordinates with centre $O_2(\rho_0,\beta)$ and semi-axes:

$$
\begin{cases}
R(\phi,t) = R_0(t)\sigma(\phi,t) \\
Z(\phi,t) = Z_0(t)\sigma(\phi,t) \\
[\sigma(r,t)]^2 = 1 - \dfrac{\phi^2}{[\phi_0(t)]^2}
\end{cases}
$$

Actually the field is not uniform inside the coil, as it was previously discussed, so in the real model the normal zone volume is considered to be the sum of 4 quarters of different surfaces like the (29) but with different axes. Let's consider, in fact, the cross section of the magnet at $\phi=0$: due to the different value of the magnetic field, the normal zone propagates faster towards the inner radius than towards the outer radius, so, referring to Fig. 5b, OA>OC and for the same reason OD>OB.

Being v_{ri} and v_{re} the quench radial velocity towards the internal and the external radius respectively and v_{au} and v_{ad} the axial quench velocity towards the top and the bottom of the coil, the ellipse semi-axes are:
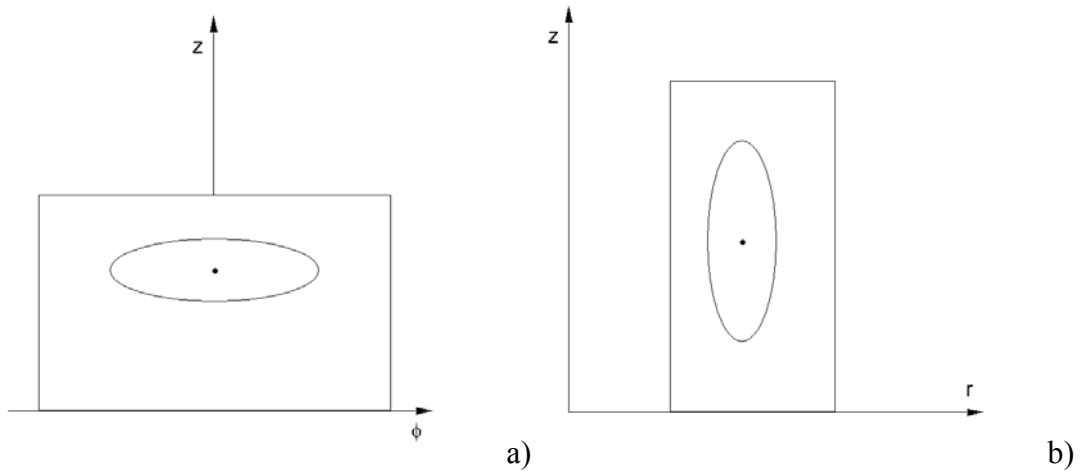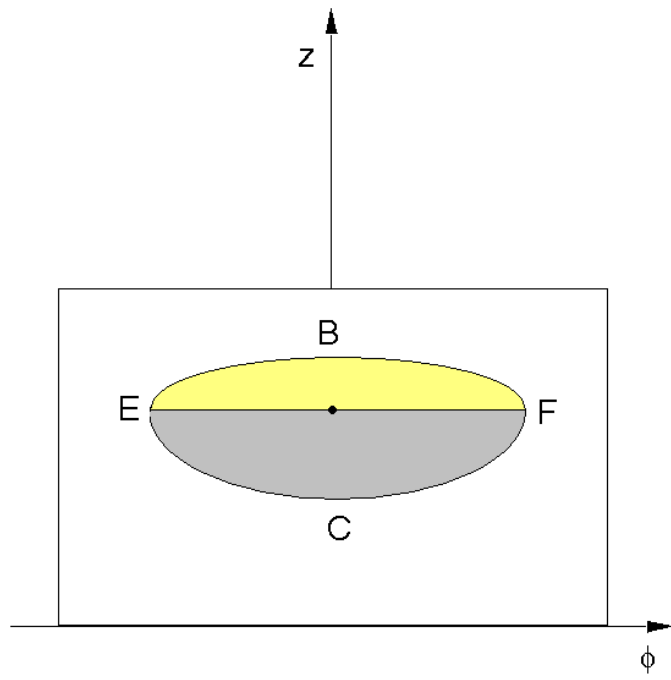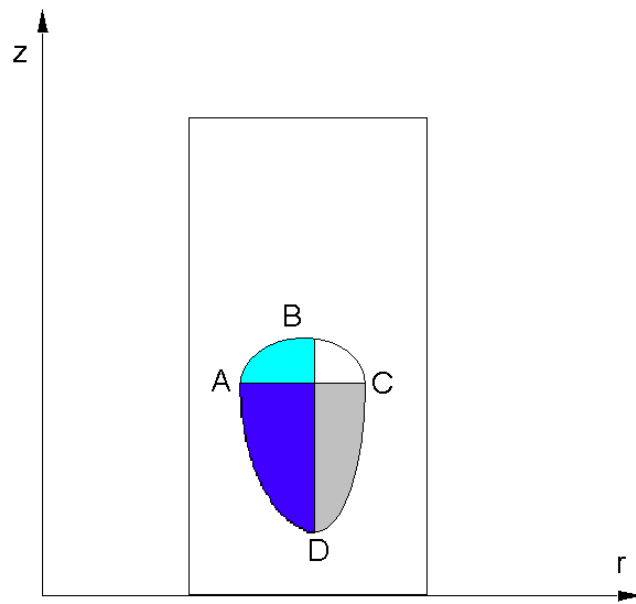

FIG. 4: Normal zone at fixed radius (a) and at fixed angle (b)

a)

b)

FIG. 5: Asymmetry of the normal zone volume at fixed radius (a) and at fixed angle (b)

$$OB = hu = \sum_{k=0}^{I} v_{au}(k) \cdot dt$$

$$OD = hd = \sum_{k=0}^{I} v_{ad}(k) \cdot dt$$

$$OA = Ri = \sum_{k=0}^{I} v_{ri}(k) \cdot dt$$

$$OC = Re = \sum_{k=0}^{I} v_{re}(k) \cdot dt$$

With this position the code can compute the evolution of a quench started at any point of the winding.

Since each magnet can be supplied with several voltage taps sectioning the coil at different radii and axial position, it's very important that the program is able to evaluate not only the total resistive volume inside the coil but also the volume of the quenched zone between adjacent taps. The normal zone calculation is achieved by evaluating at first the area $S(r)$ at a fixed radius r using cylindrical coordinates, then the volume for $a \leq r \leq b$ is obtained by integration:

$$V = \int_{a}^{b} S(r) r \, dr \tag{30}$$

As it has been remarked $S(r)$ has to be considered as the sum of two half ellipses $S(r)=Su(r)+Sd(r)$ being $Su(r)$ the upper part and $Sd(r)$ the lower area in Fig. 5a. Several different geometric situations must be taken in account in order tu evaluate $Su(r)$. As the same considerations can be done for $Sd(r)$, only the volume for the upper half ellipse will be worked out.
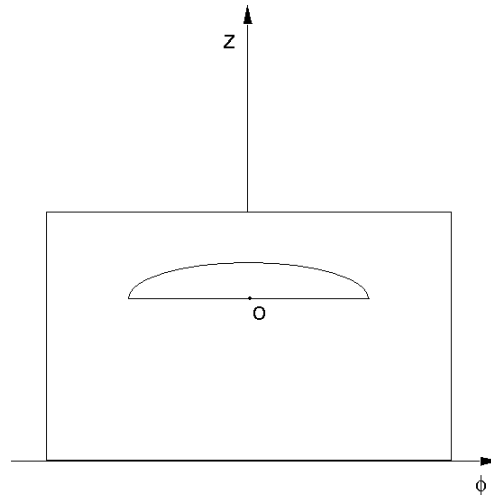
3.6.1 Case 1: Fig. 6

FIG. 6: Normal zone shape in case 1

$$\begin{cases} hu(r) = hu \cdot \alpha(r) \\ \phi(r) = \phi_0 \cdot \alpha(r) \\ hu(r) \le Hm - \beta \\ \phi(r) \le \pi \end{cases}$$

In this case it will be:

$$Su(r) = \frac{1}{2}\pi hu(r)\phi(r) = \frac{1}{2}\pi hu\alpha(r)\phi_0\alpha(r) = \frac{1}{2}hu\phi_0\alpha^2(r)$$

and the volume for $a \le r \le b$

$$V = \frac{1}{2}\int_a^b Su(r)rdr$$

$$V = \frac{\pi Z_0\phi_0}{2R^2}\left[(R^2 - \rho_0^{\,2})\frac{r^2}{2} + \frac{2}{3}\rho_0 r^3 - \frac{1}{4}r^4\right]_a^b \tag{31}$$

It has to be remarked that $R=Ri$ if $Rin \le a \le r \le b \le \rho_0$ while $R=Re$ if $\rho_0 \le a \le r \le b \le Rout$; this fact will be hereafter implied.
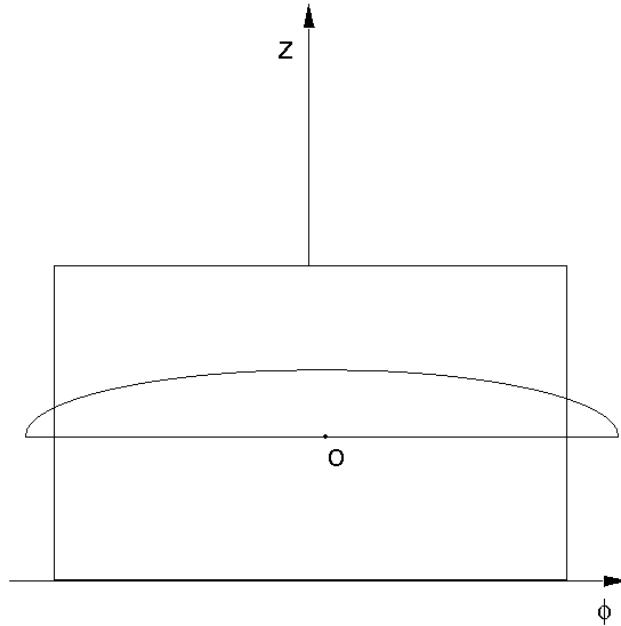
3.6.2 Case 2: Fig. 7.

FIG. 7: Normal zone shape in case 2

$$\begin{cases} hu(r) = hu \cdot \alpha(r) \\ \phi(r) = \phi_0 \cdot \alpha(r) \\ hu(r) \le Hm - \beta \\ \phi(r) > \pi \end{cases}$$

Setting $\xi = z - \beta$ the equation for the ellipse a r fixed is:

$$\frac{\xi^2}{[Z_0 \alpha(r)]^2} + \frac{\phi^2}{[\phi_0 \alpha(r)]^2} = 1 \tag{32}$$

from which:

$$\xi(\phi) = \mp Z_0 \cdot \alpha(r) \cdot \sqrt{1 - \frac{\phi^2}{[\phi_0 \alpha(r)]^2}}$$

$$Su(r) = 2 \int_0^\pi \xi(\phi) d\phi$$

$$Su(r) = hu \phi_0 \alpha^2(r) \left\{ \frac{\pi}{\phi_0 \alpha(r)} \sqrt{1 - \left(\frac{\pi}{\phi_0 \alpha(r)}\right)^2} - ar\cos\left(\frac{\pi}{\phi_0 \alpha(r)}\right) + \frac{\pi}{2} \right\}$$

The volume is obtained by numerical integration using the subroutine SIMPS.

3.6.3 Case 3: Fig. 8

$$\begin{cases} hu(r) = hu \cdot \alpha(r) \\ \phi(r) = \phi_0 \cdot \alpha(r) \\ hu(r) > Hm - \beta \\ \phi(r) \le \pi \end{cases}$$

From the equation (32), which describes the normal zone boundary at fixed radius it is possible to obtain:

$$\phi(\xi) = \mp \phi_0 \cdot \alpha(r) \cdot \sqrt{1 - \frac{\xi^2}{[Z_0 \alpha(r)]^2}} \tag{33}$$

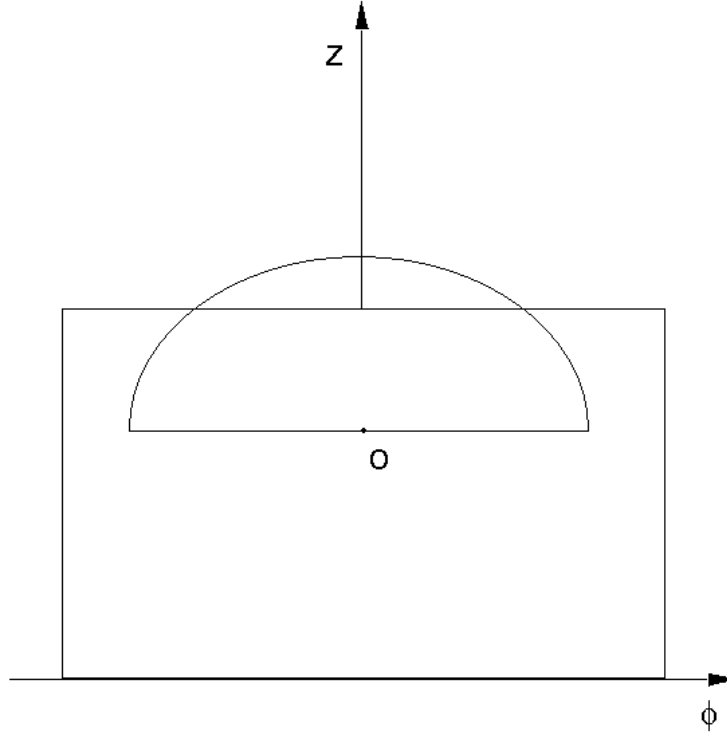**FIG. 8:** Normal zone shape in case 3

The surface *Su(r)* can then be obtained by integration

$$Su(r) = 2\int_0^{Hm-\beta} \phi(\xi)d\xi$$

$$\begin{cases} Su(r) = Z_0\phi_0\left[K\sqrt{1-K^2} - ar\cos K + \dfrac{\pi}{2}\right]\alpha^2(r) \\ \\ K = \dfrac{Hm-\beta}{Z_0\alpha(r)} \end{cases} \qquad (34)$$

Also in this case the volume is obtained by numerical integration using the subroutine SIMPS.
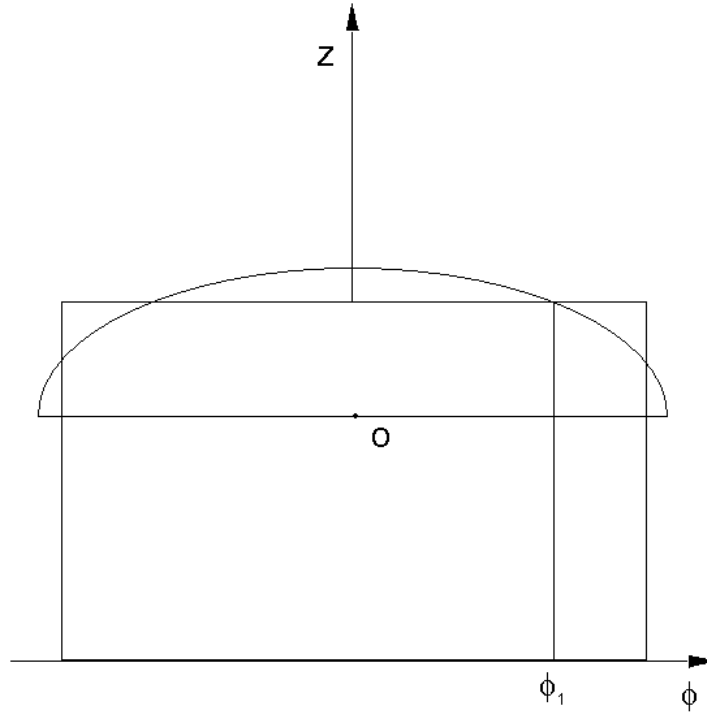
3.6.4 Case 4: Fig. 9

FIG. 9: Normal zone shape in case 4

Let's now consider the case in which the axes of the ellipse have reached the borders of the coil but there are some superconducting zone left; the normal zone will grow and when the ellipse passes through the point $T(\pi,Hm)$ the whole magnet will be in the resistive state. For $hu>Hm-\beta$ and $\phi_0>\pi$ let's find at which value of r the ellipse passes through T.

Replacing in the (29) $\phi=\pi$ and $z=Hm$ we obtain:

$$\frac{(r-\rho_0)^2}{R_0{}^2}+\frac{(Hm-\beta)^2}{Z_0{}^2}+\frac{\pi^2}{\phi_0{}^2}=1$$

and then

$$r=\rho_0\mp R_0\sqrt{1-\frac{(Hm-\beta)^2}{Z_0{}^2}-\frac{\pi^2}{\phi_0{}^2}}=\rho_0\mp R_0\sqrt{\Psi}$$

Setting

$$R_{\lim i}=\rho_0-R_0\sqrt{\Psi}$$
$$R_{\lim e}=\rho_0+R_0\sqrt{\Psi}$$

the situation sketched in Fig. 9 is described by the conditions:

$$\begin{cases} hu(r) > Hm - \beta \\ \phi(r) > \pi \\ r \leq R_{\lim i} \, or R_{\lim e} \leq r \end{cases}$$

Su(r) is obtained from:

$$Su(r) = 2\left\{\phi_1 \cdot (Hm - \beta) + \int_{\phi_1}^{\pi} Z_0 \cdot \alpha(r)\sqrt{1 - \frac{\phi^2}{[\alpha(r)\phi_0]^2}}\,d\phi\right\} \tag{35}$$

$$\begin{cases} Su(r) = 2\phi_1(Hm - \beta) + Z_0\phi_0\alpha^2(r)\left\{\gamma(r)\sqrt{1-\gamma^2} - a\cos[\gamma(r)] - \delta(r)\sqrt{1-\delta^2(r)} + a\cos[\delta(r)]\right\} \\ \gamma(r) = \dfrac{\pi}{\alpha(r)\phi_0} \\ \delta(r) = \dfrac{\phi_1}{\alpha(r)\phi_0} \end{cases}$$

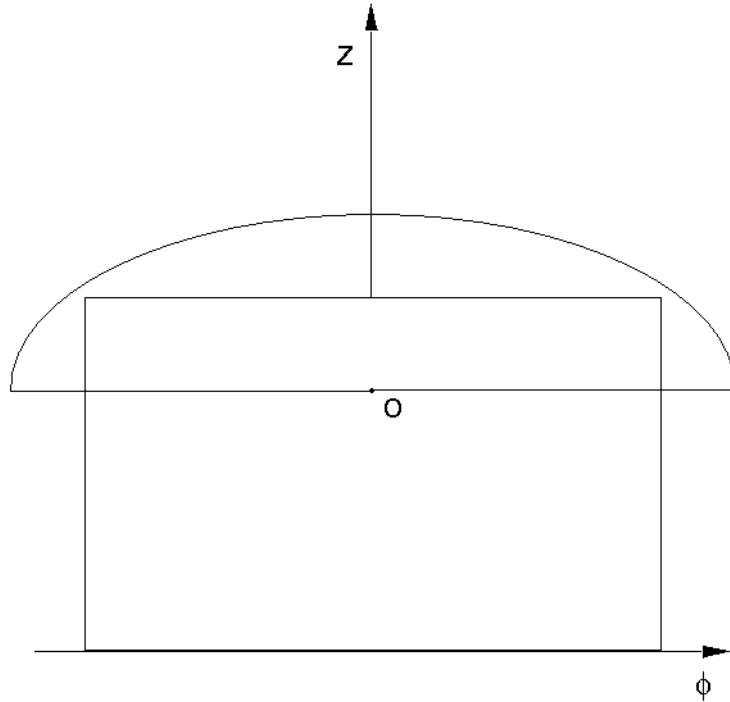*3.6.5 Case 5: Fig. 10*

FIG. 10: Normal zone shape in case 5

The last possible situation is when all the superior part of the coil is quenched, that means:

$$\begin{cases} hu(r) > Hm - \beta \\ \phi(r) > \pi \\ R_{\lim i} < r < R_{\lim e} \end{cases}$$

In this case it's simply:

$$S(r) = 2\pi (Hm - \beta)$$

$$V = \int_a^b 2\pi (Hm - \beta)r dr = \pi (b^2 - a^2)(Hm - \beta)$$

It's important to remark that in integrating in radial dimension inside a zone of the magnet, the shape of S(r) may change from situation 1 to case 5. In order to take this fact in account, the program compares the length of the axes of the ellipses at $r=a$ and $r=b$ with the dimension of the coil at the same radii and states, in this way, which is S(r) at the borders of the zone taken in account. If S(a) and S(b) have the same shape, the volume is calculated by a simple integration, otherwise the radii at which it changes, are evaluated and the volume is obtained as sum of parts inside of which the shape of S(r) is the same.

3.7 Resistance

When the normal zone volume V is known for each zone, the resistance R is obtained by

$$R = \rho_v(B,\Theta) \cdot V \tag{36}$$

where ρ_v is the resistance per volume unit of the magnet, i.e.:

$$\rho_v(B,\Theta) = \frac{\rho_{av}(B,\Theta)}{S^2}$$

where $\rho_{av.}$ is the average resistivity (see paragraph 3.5.3) and S the unit cell area.
The magnetic field affecting the resistivity of metals is assumed to be the average over the total resistive zone:

$$B_{av} = \frac{B_A + B_B + B_C + B_D + B_O}{5} \tag{37}$$

where A, B, C, D, o are the point in Fig. 5b.

As far as the temperature is concerned, we must remember that it isn't uniform inside the normal zone. During the first time step δt the normal zone grows up to V_1 and warms up to $\Theta=\Theta_1$ because of ohmic dissipation. During the second time step, the resistive zone reaches V_2 so V_1 has to be heated for $2 \cdot \delta t$ up to Θ_2, while V_2-V_1 has been heated only for δt. In this way the normal zone at the N-th temporal step is conceived like N concentric shells, each one at a different temperature Θ_i^N such as $\Theta_i^N > \Theta_{i+1}^N$ for $i=1,\dots$, N-1.

The normal zone resistance at the N-th temporal step is so calculated as:

$$R = \sum_{k=1}^{N} \rho_v(B_{av}^N, \Theta_k^N) \cdot \Delta V_k$$

where B_{av}^N is the averaged field from (37) at the N-th time step and ΔV_k is the normal zone volume increment during the k-th time step.

3.8 Temperature

The temperature of each shell is obtained by solving the thermal balance equation under the hypothesis of local adiabaticity, that is:

$$\rho(\Theta)J^2(t)dt = \gamma C(\Theta)d\Theta \tag{38}$$

In the program the approximation is that $J(t)$ is constant in each temporal step; consequently eq. (38) becomes:

$$\frac{d\Theta}{dt} = J^2 \frac{\rho(\Theta)}{\gamma C(\Theta)} \tag{39}$$

It's important to notice that since ρ is the effective resistivity of the whole cell, J is here the overall current density, i.e. J=J$_{overall}$=I/S$_{cell}$.

When the temperature Θ is between Θ_g and Θ_c, the term J^2 in the right hand of eq. (39) is substituted by:

$$J \cdot [J - J(B,\Theta)] \tag{40}$$

where $J(B,\Theta)$ is the critical current density at the B and Θ. In this way the condition of linearity of the generation function with the temperature is fulfilled when $\Theta_g \leq \Theta \leq \Theta_c$, as normally is assumed (paragraph 5.4 of [1]).

The eq. (39) is to be solved for all the N layers; each one is increasing in temperature without heat exchange with the cryogenic bath or the adjacent layers (*adiabatic hypothesis*). The differential eq. (39) is integrated using the Runge-Kutta of 4-th order method, i.e. the temperature Θ_i of each shell at the i-th step assumes the following value:

$$
\begin{cases}
\Theta_i = \Theta_{i-1} + \dfrac{1}{6}\left(\delta\Theta_1 + \delta\Theta_2 + \delta\Theta_3 + \delta\Theta_4\right) \\[2mm]
\delta\Theta_1 = J_{i-1}{}^2 \dfrac{\rho(\Theta_{i-1})}{\gamma C(\Theta_{i-1})}\delta t \\[2mm]
\delta\Theta_2 = J_{i-1}{}^2 \dfrac{\rho(\Theta_{i-1} + \delta\Theta_1)}{\gamma C(\Theta_{i-1} + \delta\Theta_1)}\delta t \\[2mm]
\delta\Theta_3 = J_{i-1}{}^2 \dfrac{\rho(\Theta_{i-1} + \delta\Theta_2)}{\gamma C(\Theta_{i-1} + \delta\Theta_2)}\delta t \\[2mm]
\delta\Theta_4 = J_{i-1}{}^2 \dfrac{\rho(\Theta_{i-1} + \delta\Theta_3)}{\gamma C(\Theta_{i-1} + \delta\Theta_3)}\delta t
\end{cases}
\tag{41}
$$

where δt is the time step, ρ and C are averaged over the unit cell, and $J_{i-1}{}^2$ is the square of the current density at the i-1 –th temporal step or the expression (40) if $\Theta_g \leq \Theta_{i-1} \leq \Theta_c$. Because of numerical errors, it could happen that the term of eq. (41)

$$
\frac{1}{6}\left(\delta\Theta_1 + \delta\Theta_2 + \delta\Theta_3 + \delta\Theta_4\right)
\tag{42}
$$

increases too fast, especially at low temperature, where the quantity C is very small and has a strong dependence on T. The cure might be a very short time integration step, at least at the beginning when the thermal inertia is very small, but then it would be very inconvenient all along the computation run, generating very heavy matrixes and heavy output files. In order to avoid this situation and to face this problem with some a way that has a physical significance, the (42) is compared with a quantity controlled by the user (the name in the input file is *deltemp*): if it exceeds *deltemp*, the temporal step δt is divided by 2, and the eq. (41) is again applied for this reduced temporal step. If the new quantity (42), obtained with a lower δt, results again higher than *deltemp*, δt is divided by 3 and the operation is iterated so on. Somehow *deltemp* is the temperature step over which is consistent to assume constant value for the important physical parameters.

3.9   Current equation

3.9.1 *Circuit in* driven *mode (*DRV*)*

The equations for current evaluation depend on the electrical circuit configuration that may change during a quench event. Let's first examine the simple case of one coil and we shall extend later to the case of many coils connected in series, finally to the case of many coils with different power supplies and independent dumping resistors.

Let's now discuss the possible electric connection of one coil to the room temperature circuit.

3.9.1.1 Case 1: $t < \tau_d$, $V < V_{max1}$, $I = I_0$

Any sort of quench detection system (QDS) doesn't break the current supply off instantaneously but after a delay time τ_d; so for $t_0 \leq t \leq \tau_d$ the power supply provides a constant current. At this level we assume that the dynamic range of the power supply is such to stay in current mode despite the increasing voltage. Actually τ_d is the total time required by the QDS both to recognize the start of a quench and the electronic delay before the circuit starts to open. Its value is given in the input file with the name *deltime*.

Due to the growing of the resistive zone, current begins to share between magnet and dump resistor, and a voltage, which is the sum of a resistive and of an inductive signal, is present at the different voltage taps.
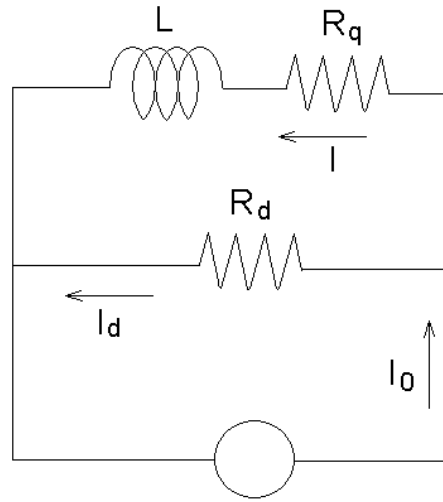

FIG. 11: Electric circuit of one quenched coil while still in current mode

During this time the circuit describing one quenched coil is the one in Fig. 11 and the equations for the current in the circuit are:

$$\begin{cases} R_q I + L\dfrac{dI}{dt} - R_d I_d = 0 \\ I_0 = I + I_d \end{cases} \tag{42}$$

from which we obtain

$$L\frac{dI}{dt} = -\left(R_d + R_q\right)I + R_d I_0$$

and then setting $R_T = R_d + R_q$ we have

$$L\frac{dI}{dt} = -R_T I + R_d I_0$$

If we consider *Nc* coupled coils, each one independently supplied and each one in the configuration of Fig. 11, the equations for the *n*-th of them are:

$$\begin{cases} R_{qn}I + \sum_{j=1}^{N_c} M_{n,j}\frac{dI_j}{dt} - R_{dn}I_{dn} = 0 \\ I_{0n} = I_n + I_{dn} \end{cases} \tag{43}$$

where $M_{n,j}$ is the mutual inductance between the n-th and the j-th coil. The (43) can be rewritten as:

$$\sum_{j=1}^{N_c} M_{n,j}\frac{dI_j}{dt} = -R_{Tn}I_n + R_{dn}I_{0n} \tag{44}$$

3.9.1.2 Case 2: $t < \tau_d$, $V_{max1} \le V \le V_{max2}$

Before the opening of the circuit, it may happen that the total voltage across the coil exceeds the maximum value V_{max2} that the power supply can deliver. In this case, the current supply will switch from current mode to voltage mode. As a matter of fact, no real power supply can reach the maximum voltage V_{max2} and suddenly switch to voltage mode: actually at a voltage $V_{max1} \le V_{max2}$ the delivered current start decreasing and the maximum value V_{max2} is smoothly achieved. It is possible to describe the transition from current to voltage mode as a power supply providing a voltage $V=V(t)$ increasing in time from V_{max1} to V_{max2}; in this case the circuit equations are:

$$\begin{cases} R_q I + L\frac{dI}{dt} - R_d I_d = 0 \\ V = V(t) = R_d I_d \end{cases} \tag{45}$$

from which we obtain:

$$L\frac{dI}{dt} = V(t) - R_q I \tag{46}$$

It's very difficult to predict the real shape of $V=V(t)$, which depends on the type and quality of the power supply; so two different equations have been worked out from comparing

simulation and experimental data. The user can choose the one he wants to use by setting in input the parameter *ivt* equal to 1 or 2.

In the first case (*ivt=1*) *V(t)* is assumed to be:

$$V(t) = A \cdot \exp\left[-\frac{(\tau_v - t)^2}{K} \right] \tag{47}$$

τ_v is the time at which the voltage V_{max2} is reached and its value must be input like the values for V_{max1} and V_{max2} (*tau, Vmax1* and *Vmax2* respectively), while A and K are obtained by imposing the following conditions:

➤ Replacing $t = \tau_v$ in the (47) it mast be $V(\tau_v) = V_{max2}$ from which we have:

$$A = V_{max1}$$

➤ If t_1 is the time at which the voltage is $V = V_{max1}$ then it has to be:

$$V_{max1} = V_{max2} \cdot \exp\left[-\frac{(\tau_v - t_1)^2}{K} \right]$$

from which we get

$$K = \frac{(\tau_v - t_1)^2}{\ln\dfrac{V_{max2}}{V_{max1}}} \tag{48}$$

The second possible choice (*ivt=2*) for *V(t)* is:

$$V(t) = A(t - \tau_v)^{2n} + B \tag{49}$$

The values for the parameters *A* and *B* are obtained by imposing the same conditions as in the previous case, i.e. $V(\tau_v) = V_{max2}$ and $V(t_1) = V_{max1}$. In this case we obtain:

$$V(t) = \frac{V_{max1} - V_{max2}}{(t_1 - \tau_v)^{2n}} (t - \tau_v)^{2n} + V_{max2} \tag{50}$$

The parameter *n* must be input by the user (*ind* in the input file).
In the more general case of *Nc* coupled coils the (46) is replaced for the *n*-th magnet by:

$$\sum_{j=1}^{N_c} M_{n,j} \frac{dI_j}{dt} = V_n(t) - R_{qn}I_n \tag{51}$$

If $V_{max1} = V_{max2}$ the transition of the power supply from current mode to voltage mode is sharp; in such a case the program steps from case 1 to case 3.

3.9.1.3 Case 3: $t < \tau_d$, $V \geq V_{max2}$
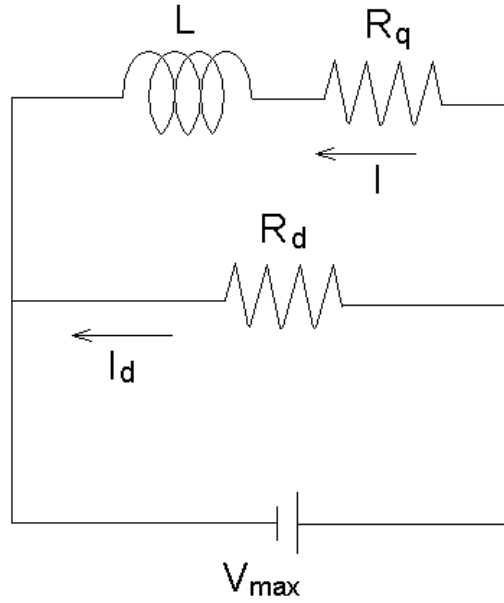
FIG. 12: The quenched coils are supplied in voltage mode

If the maximum voltage V_{max2} has been reached and the power supply is not already off, i.e. $t \leq \tau_{del}$, the circuit is like the one in Fig. 12 and the equations for the current are:

$$\begin{cases} R_q I + L\dfrac{dI}{dt} - R_d I_d = 0 \\ V_{max2} = R_d I_d \end{cases}$$

(52)

$$L\frac{dI}{dt} = V_{max2} - R_q I$$

(53)

or for the *n*-th of *Nc* coupled coils:

$$\sum_{j=1}^{N_c} M_{n,j} \frac{dI_j}{dt} = V_{\max 2n} - R_{qn} I_n \tag{54}$$

3.9.1.4 Case 4: $\tau_d \leq t < \tau_d + \tau_{arc}$

When the switch activated by the QDS opens the circuit, the current doesn't go down abruptly to zero but flows through an arc for a time τ_{arc} (*timarc* in the input file) until the arc itself is extinguished. It is possible to schematize with a power supply providing a current $I_0(t)$ decreasing from $I_0(\tau_d)$ to zero in the time τ_{arc}. The circuit describing this situation is the same as Fig. 11, and the following equations hold:

$$\begin{cases} R_q I + L \dfrac{dI}{dt} - R_d I_d = 0 \\ I_0(t) = I + I_d \end{cases} \tag{55}$$

As it was previously discussed for *V(t)* in the situation 2, the time dependence of $I_0(t)$ is not known a priori. Again we use a dependence on time that, among the ones we tested, fits well our experimental data:

$$I_0(t) = I_0 \cos^2\left(\frac{\pi}{2} \cdot \frac{t - \tau_d}{\tau_{arc}} \right)$$

From the (55) we obtain:

$$L \frac{dI}{dt} = -R_T I + R_d I_0(\tau_d) \cos^2\left(\frac{\pi}{2} \cdot \frac{t - \tau_d}{\tau_{arc}} \right) \tag{56}$$

and for the general case of *Nc* coupled coils:

$$\sum_{j=1}^{N_c} M_{n,j} \frac{dI_j}{dt} = -R_{Tn} I_n + R_{dn} I_{0n}(\tau_{dn}) \cos^2\left(\frac{\pi}{2} \cdot \frac{t - \tau_{dn}}{\tau_{arc(n)}} \right) \tag{57}$$

3.9.1.5 Case 5: $t \geq \tau_d + \tau_{arc}$

At the end, when the power supply is definitively off, we'll have the simple R-L circuit sketched in Fig. 13 and described by the:

$$\begin{cases} R_q I + L \dfrac{dI}{dt} - R_d I_d = 0 \\ I + I_d = 0 \end{cases} \tag{58}$$

from which we have:

$$L \frac{dI}{dt} = -R_T I \tag{59}$$
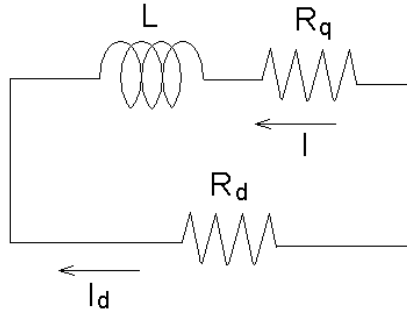
FIG. 13: Electric circuit after the power supply has been disconnected

And for the *n*-th of *Nc* coupled windings:

$$\sum_{j=1}^{N_c} M_{n,j} \frac{dI_j}{dt} = -R_{Tn} I_n \tag{60}$$

Let's now consider *Nc* coupled coils each one independently supplied: the whole system is described by *Nc* coupled equations which ca be written in matrix form as:

$$\underline{\underline{M}} \, \underline{\dot{I}} = \underline{VETT} \tag{61}$$

where it may be:

$$VETT(n) = -R_{Tn} I_n + R_{dn} I_{0n}$$
$$VETT(n) = V_n(t) - R_{qn} I_{0n}$$

$$VETT(n) = V_{\max 2n} - R_{qn} I_{0n}$$

$$VETT(n) = -R_{Tn} I_n + R_{dn} I_{0n} \cos^2\left(\frac{\pi}{2} \cdot \frac{t - \tau_{dn}}{\tau_{arc(n)}}\right)$$

$$VETT(n) = -R_{Tn} I_n$$

depending on the state of the n-th coil at the considered time.

At last, in order to be able to simulate the quench effects in a quite general situation, we have to describe what are the equations to be used when some magnets are connected in series each other. Let's so consider the circuit in Fig. 14 where there are two coils in series to each other an in parallel with a dump resistor R_d.
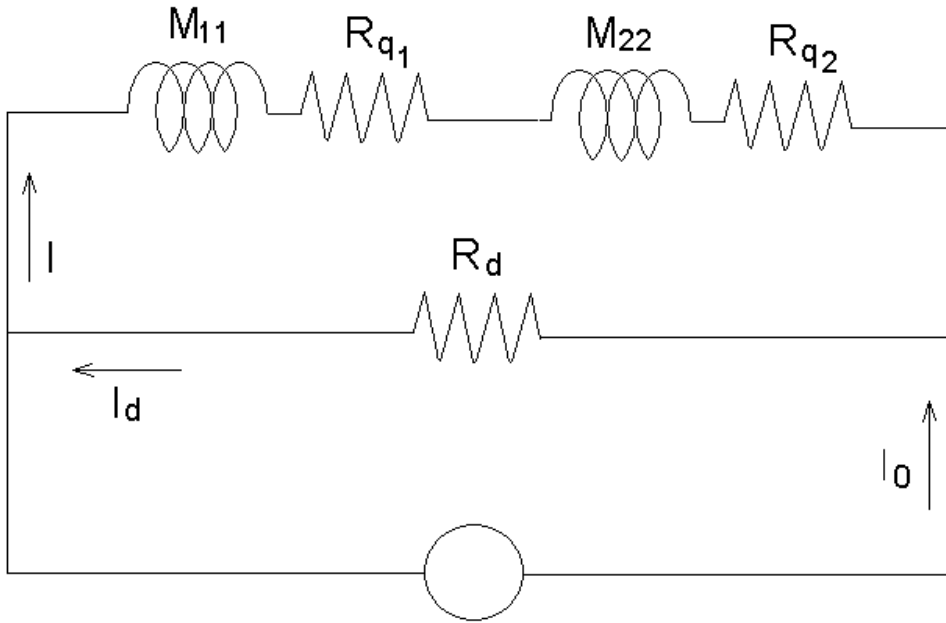

FIG. 14: Electric circuit when two coil are supplied in series

The first equation of (45) in this case is:

$$(L_1 + L_2 + 2M_{1,2})\frac{dI}{dt} + (R_{q1} + R_{q2})I = R_d I_d$$

If there were Ns coils connected in series, we would have:

$$\left(\sum_{i,j} M_{i,j}\right)\frac{dI}{dt}+\left(\sum_{k=1}^{Ns} R_{qk}\right)I = R_d I_d$$

So we can say that a circuit of *Ns* coils all connected in series is equivalent to a circuit with only one magnet whose inductance and resistance respectively are:

$$L = \sum_{i,j} M_{i,j}$$

$$R_q = \sum_{k=1}^{Ns} R_{qk}$$

In this way the (61) can still be used only replacing L and R_q.

3.9.2 *Circuit in* persistent *mode (*PER*)*

Normally the magnets working in persistent mode have shunt resistors across terminals for the protection of the coils and they are connected to the power supply only during the charge or discharge of the magnet. The program foresees the simulation of the quench both when the magnet is in persistent mode and when it is connected with the power supply. We will see that the first case is a particular case of the second, with some suitable values for some parameters; consequently we begin to present the circuit when it is connected to the power supply. Also in this case the power supply is limited in tension by the parameters V_{max1} and V_{max2} and there is a QDS for the detection of a quench with a delay time τ_d for the opening of the main switch and with an arc time τ_{arc} for the extinguishing of the arc, exactly like for the *driven* mode that has been presented in the previous paragraphs. In this case many coils can be connected in series, each one with its own shunt resistor, but only one power supply, with a dump resistor in parallel, is admitted in the circuit (see Fig. 15).

3.9.2.1 *Case 1:* $t < \tau_d$, $V < V_{max1}$, $I = I_0$

For $t_0 \le t \le \tau_d$ the power supply provides a constant current. Also in this case τ_d is the total time required by the QDS both to recognize the start of a quench and the electronic delay before the circuit starts to open.

Due to the growing of the resistive zone, current begins to share between magnets and dump resistor, and a voltage, which is the sum of a resistive and of an inductive signal, is present at the different voltage taps.
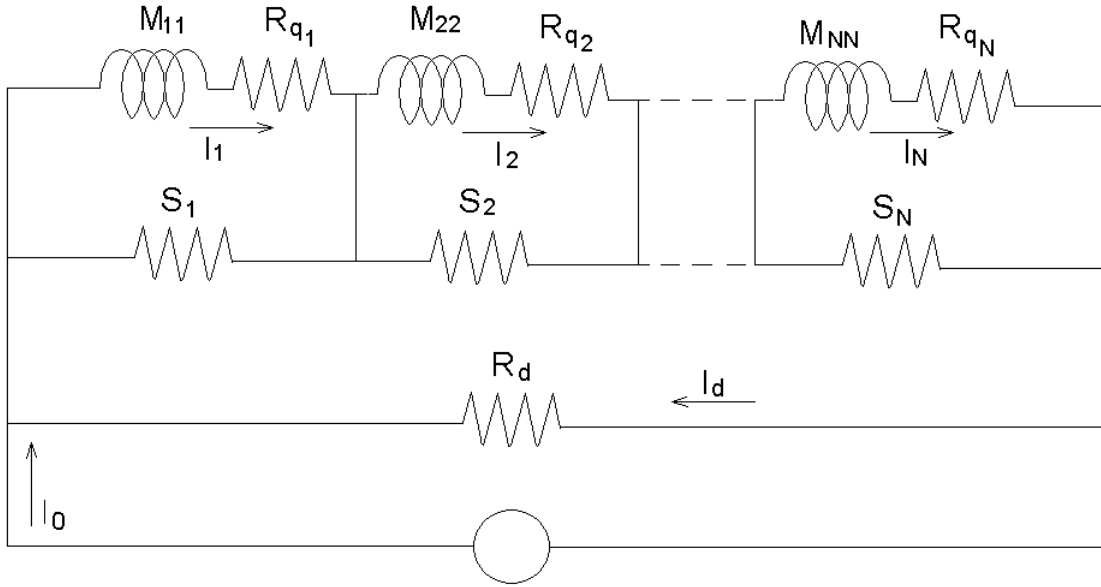
FIG. 15: Electric circuit of magnet in *persistent* mode with the power supply still in current mode

The circuit describing the magnet is the one in Fig. 15 and the equations for the current in the circuit are:

$$\begin{cases} (I_1 - I_d)S_1 + R_{q1}I_1 + \sum_{i=1}^{N} M_{1,i} \dfrac{dI_i}{dt} = 0 \\[2mm] (I_2 - I_d)S_2 + R_{q2}I_2 + \sum_{i=1}^{N} M_{2,i} \dfrac{dI_i}{dt} = 0 \\[2mm] \dotfill \\[1mm] (I_N - I_d)S_N + R_{qN}I_N + \sum_{i=1}^{N} M_{N,i} \dfrac{dI_i}{dt} = 0 \\[2mm] \sum_{i=1}^{N} (I_d - I_i)S_i + (I_d - I_0)R_d = 0 \end{cases} \qquad (62)$$

from the last one we obtain:

$$I_d = \frac{\sum I_i S_i + I_0 R_d}{\sum S_i + R_d}$$

and consequently for each one of the first N equation of (62) we obtain:

$$\sum_{i=1}^{N} M_{n,i} \frac{dI_i}{dt} = S_n \frac{\sum I_i S_i + I_0 R_d}{\sum S_i + R_d} - (R_n + S_n)I_n \tag{63}$$

3.9.2.2 Case 2: $t < \tau_d$, $V_{max1} \leq V \leq V_{max2}$

Before the opening of the circuit, it may happen that the total voltage across the coils exceeds the maximum value V_{max2} that the power supply can support. In this case, the current supply will switch from current mode to voltage mode. As a matter of fact, no real power supply can reach the maximum voltage V_{max2} and suddenly switch to voltage mode: actually at a voltage $V_{max1} \leq V_{max2}$ the delivered current start decreasing and the maximum value V_{max2} is smoothly achieved. It is possible to describe the transition from current to voltage mode as a power supply providing a voltage $V=V(t)$ increasing in time from V_{max1} to V_{max2}; in this case the circuit equations are:

$$\begin{cases} (I_1 - I_d)S_1 + R_{q1}I_1 + \sum_{i=1}^{N} M_{1,i} \frac{dI_i}{dt} = 0 \\ (I_2 - I_d)S_2 + R_{q2}I_2 + \sum_{i=1}^{N} M_{2,i} \frac{dI_i}{dt} = 0 \\ \qquad\cdots\cdots\cdots \\ (I_N - I_d)S_N + R_{qN}I_N + \sum_{i=1}^{N} M_{N,i} \frac{dI_i}{dt} = 0 \\ \qquad (I_d - I_0)R_d = V(t) \end{cases} \tag{64}$$

from the last one we obtain:

$$I_d = \frac{\sum I_i S_i + V(t)}{\sum S_i} \tag{65}$$

consequently for the *n*-magnet:

$$\sum_{i=1}^{N} M_{n,i} \frac{dI_i}{dt} = S_n \frac{\sum I_i S_i + V(t)}{\sum S_i} - (R_n + S_n)I_n \tag{66}$$

The expression of *V(t)* is the same of the one presented in paragraph 3.9.1.2 with eq. (47) or (49). Consequently also in this case the user can choose to select the model for *V(t)* by setting in input the parameter *ivt* equal to 1 or 2.

If $V_{max1} = V_{max2}$ the transition of the power supply from current mode to voltage mode is sharp; in such a case the program steps from case 1 to case 3.

3.9.2.3 Case 3: $t < \tau_d$, $V \geq V_{\max 2}$

If the maximum voltage $V_{\max 2}$ has been reached and the power supply is not already off, i.e. $t \leq \tau_{del}$, the equations for the current are the same of (64), (65) and (66) with $V(t) = V_{\max 2}$.

3.9.2.4 Case 4: $\tau_d \leq t < \tau_d + \tau_{arc}$

When the switch activated by the QDS opens the circuit, the current doesn't go down abruptly to zero but flows through an arc for a time τ_{arc} until the arc itself is extinguished. It is possible to schematize with a power supply providing a current $I_0(t)$ decreasing from $I_0(\tau_d)$ to zero in the time τ_{arc}. The circuit describing this situation is the same as Fig. 15, and the same equations (62) and (63) hold, with the difference that now the I_0 is not constant but $I_0 = I_0(t)$. The function $I_0(t)$ has been already described in paragraph 3.9.1.4.

3.9.2.5 Case 5: $t \geq \tau_d + \tau_{arc}$

At the end, when the switch is definitively open, we'll have the circuit sketched in Fig. 16 and described by the following equations:

$$
\begin{cases}
(I_1 - I_d)S_1 + R_{q1}I_1 + \sum_{i=1}^{N} M_{1,i} \dfrac{dI_i}{dt} = 0 \\[2mm]
(I_2 - I_d)S_2 + R_{q2}I_2 + \sum_{i=1}^{N} M_{2,i} \dfrac{dI_i}{dt} = 0 \\[2mm]
\cdots\cdots\cdots \\[2mm]
(I_N - I_d)S_N + R_{qN}I_N + \sum_{i=1}^{N} M_{N,i} \dfrac{dI_i}{dt} = 0 \\[2mm]
\sum_{i=1}^{N}(I_d - I_i)S_i + I_d R_d = 0
\end{cases}
\tag{67}
$$

from which we have:

$$
\sum_{i=1}^{N} M_{n,i} \frac{dI_i}{dt} = S_n \frac{\sum I_i S_i}{\sum S_i + R_d} - (R_n + S_n)I_n
\tag{68}
$$
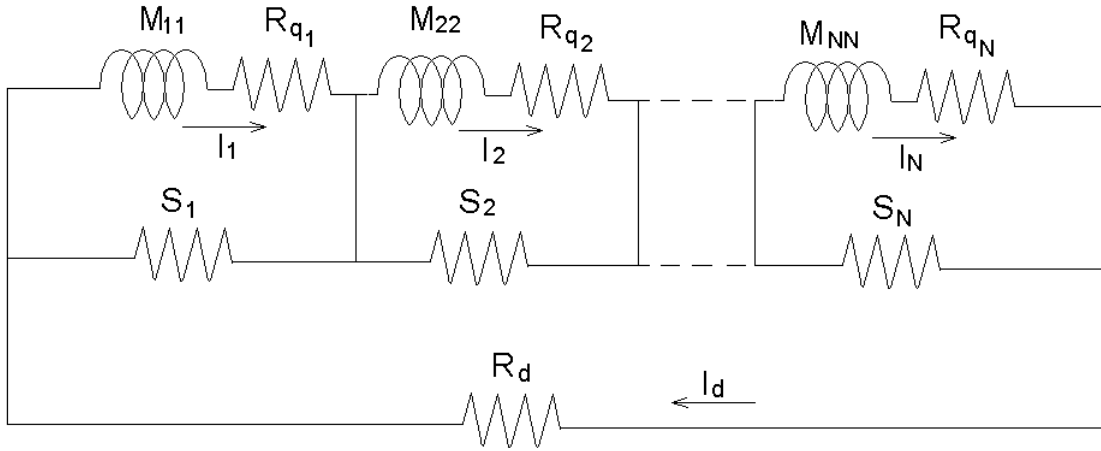
FIG. 16: Circuit with the power supply definitively off

So the system of the *N* winding can be described by a *N* coupled equations, which in matrix form can be written as:

$$\underline{\underline{M}}\,\underline{\dot{I}} = \underline{VETT} \qquad (69)$$

where for the different cases:

$$VETT(n) = S_n \frac{\sum I_i S_i + I_0 R_d}{\sum S_i + R_d} - (R_n + S_n)I_n$$

$$VETT(n) = S_n \frac{\sum I_i S_i + V(t)}{\sum S_i} - (R_n + S_n)I_n$$

$$VETT(n) = S_n \frac{\sum I_i S_i + V_{max2}}{\sum S_i} - (R_n + S_n)I_n$$

$$VETT(n) = S_n \frac{\sum I_i S_i + I_0 \cos^2\left(\frac{\pi}{2} \cdot \frac{t - \tau_{dn}}{\tau_{arc(n)}}\right) R_d}{\sum S_i + R_d}$$

$$VETT(n) = S_n \frac{\sum I_i S_i}{\sum S_i + R_d} - (R_n + S_n)I_n$$

depending on the state of the *n*-th coil at the considered time.

The case with the magnet working in persistent mode can be easily simulated by the situation with the power supply, with a sufficiently high value for τ_d and imposing $V_{max\,2} = V_{max\,1} = 0$ or/and $R_d = 0$. In this case the coils are in short circuit and they work in persistent mode.

3.10 Partial and total voltage calculation

When the current and its time derivative is known for each magnet, it's possible to evaluate the voltage across adjacent taps. In fact each coil can be subdivided in more parts in radial and axial direction. The voltage across each zone is the sum of two different terms:
1. The voltage due to resistance of the normal zone in that section;
2. The voltage due to the mutual inductance between the section taken in account and the coils (including the coil to which the section belongs).

In this way, if we have Nc coils and the n-th of them is subdivided in $N_r(n)$ parts in radial direction and $N_h(n)$ parts in axial direction, the voltage between the i-th and $(i+1)$-th radial voltage tap and the j-th and $(j+1)$-th axial voltage tap, is:

$$V_{i,j}^{(n)} = R_{qi,j}^{(n)} + \sum_{k=1}^{Nc} M_{i,j,k}^{(n)} \frac{dI_k}{dt} \tag{70}$$

where $M_{i,j,k}^{(n)}$ is the mutual inductance of the i-th radial zone, j-th axial zone of the n-th magnet with the k-th magnet (*hmuts(n,i,j,k)* in the input file).

The total voltage across the n-th magnet is obtained by adding (70):

$$V^{(n)} = \sum_{i=1}^{Nr(n)} \sum_{j=1}^{Nh(n)} V_{i,j}^{(n)} \tag{71}$$

3.11 Heat transmission in helium bath

Although this code is devoted to adiabatic magnet, we wanted to consider also the evaporation and the warming of the cryogenic liquid, even if this point is addressed with a very rough approximation. The aim is that it can happen that during a quench in a multi-coil magnet, some windings do not quench, because the induced current is never higher than the critical current and because the thermal disconnection among coils impedes the quench to propagate through solid conduction. However the helium bath is warmed by the quenched coils and, in the persistent case, by the shunt resistors that normally are inserted in the helium bath. Consequently, soon or later, all the coils will have to quench, because the temperature of the bath increases.

The energy dissipated in the helium bath is the sum of two parts:

The energy dissipated in the N shunt resistors at the i-th temporal step, which is given by:

$$E_{diss,1} = \sum_{j=1}^{N} Rs_j \left[Is_j(t_i) \right]^2 \delta t \qquad (72)$$

where Rs_j is the j-th shunt resistor, $Is_j(t_i)$ is the current in the j-th shunt at the i-th temporal step and δt is the temporal step. This term is present only in the case of *persistent* mode (*PER*)

The energy transferred by the quenched coil into the helium bath. Two options of calculation are foreseen: if the input parameter *ienergy*=1 the energy transferred by the coils at the i-th temporal step is obtained by:

$$E_{diss,2} = \sum_{j=1}^{N} \left[h_j \left(\Theta s_j - \Theta_{0i} \right) + k_j \right] S_j \delta t \qquad (73)$$

where h_j and k_j are the coefficient of thermal exchange given in the input file (*coetr* and *coeq* respectively. Typical value are: $h_j \approx 600$ Wm^{-2}K^{-1} and $k_j \approx 500$ Wm^{-2}); S_j is equivalent to the surface of a cylinder with same radius of the internal radius of the coil and with height equal to the axial axis of the normal zone ellipsoid; Θ_{0i} is the temperature of the helium bath at the i-th temporal step and Θs_j is the average temperature the normal shells of the j-th coil.

If the input parameter *ienergy*≠1, the energy transferred by each coil at the i-th temporal step is approximated in excess by:

$$E_{diss,2} = \sum_{j=1}^{N} Rq_j \left[I_j(t_i) \right]^2 \delta t \qquad (74)$$

where Rq_j is the resistance of the j-th coil and $I_j(t_i)$ the current in the j-th coil at the i-th temporal step. This means that in this case it is supposed that all the dissipated energy inside the coil is transferred to the helium bath.

The temperature Θ_{0i} of the helium bath (and consequently the operation temperature of the still superconducting coils) increases gradually at each temporal step because these energies are transferred to the bath. The helium is supposed a liquid up to 4.2 K with a specific heat of 2200 J kg^{-1}K^{-1}, the latent heat is 3200 J kg^{-1} and the specific heat of the gas is 20900 J kg^{-1}K^{-1}. The helium mass is given in the input file (*elimass*) and it is supposed to be constant during the evolution of the quench.

It is worth to underline again that these approximations for the heat transfer to the helium are very rough and the only purpose is to force all the coils to quench when a quench in a coil has been started.

3.12 Calculation of the enthalpy margin, MPZ and MQE

The code gives an evaluation of the enthalpy margin, Minimum Propagating Zone (MPZ) and Minimum Quench Energy (MQE) of each coils; these data are reported in the main output file and give to the user an evaluation of the stability of the magnet. The

calculations of MPZ and MQE are performed according the theory reported in paragraph 5.5 of [1], which we don't repeat here. We just mention the validity criteria for such results:

➢ In the calculation the coil is assumed to be an anisotropic continuum medium with different thermal conductivity in the longitudinal, radial and axial direction: the MPZ is a 3D ellipsoid with different axis in the longitudinal, radial and axial direction. As consequence this approximation will only apply in situation where the transversal dimensions of the individual conductors are less than the axis of the MPZ ellipsoid. The lengths of the axis are also reported in the main output file, so the user can easily compare them with the unit cell dimensions.

➢ The theory assumes that the time necessary to the current to diffuse into the stabilizing metal (current diffusion time) can be neglected with respect to the time required to the heat to propagate through the unit cell (heat diffusion time). Consequently the results of the code overestimate the MPZ and MQE in all the cases where this situation doesn't apply, i.e. where the stabilizing metal cross area is very large.

4. **Instruction for the preparation of the input file**

The input file is a text file with an extension ".inp". Here we report the instruction to prepare such file, with the indication to which paragraph referring for a more detailed explanation of the parameter.

4.1 Case in *driven* mode (*DRV*)

	Name of parameter	See paragr.
1.	Title of the run	4.1.1
2.	Type of circuit	4.1.2
3.	ncoil, necoil	4.1.3
4.	isc	4.1.4
5.	cosbeta	4.1.5
6.	rmin,rmax, dh	4.1.6
7.	timq, rquen, yquen, rrqui, hhqui, llqui	4.1.7
8.	nzon	4.1.8
9.	nzonh	4.1.9
10.	R(ncoil,nzon)	4.1.10
11.	d(ncoi,nzon)	4.1.11
12.	nh(ncoil, nzon, nzonh)	4.1.12
13.	ivel, the0, deltemp	4.1.13
14.	themax, bmax, xlub	4.1.14
15.	b0i,brinti,brexti,bhinti,bhexti,bexti	4.1.15
16.	num(Ic-B),alfa,beta,thecc	4.1.16
17.	Ic, B	4.1.17
18.	Nc	4.1.18
19.	mat,frac,rrr,mattype	4.1.19

20.	alr,alh,alinsr,alinsh	4.1.20
21.	vqds(ncoil,j,nzonh)	4.1.21
22.	hmuts(ncoil,nzon,nzonh,ncoil)	4.1.22
23.	amp0, rdump, ind, ivt	4.1.23
24.	timarc, deltime	4.1.24
25.	nswi	4.1.25
26.	vmax1	4.1.26
27.	vmax2	4.1.27
28.	tau	4.1.28
29.	nacc	4.1.29
30.	nts, dt, iout	4.1.30
31.	ienergy	4.1.31
32.	coetr, coeq	4.1.32
33.	elimass	4.1.33
34.	corvri,corvre,corvhu,corvhd,corvz	4.1.34
35.	tedi	4.1.35
36.	kvl	4.1.36
37.	acu	4.1.37
38.	adif	4.1.38
39.	difle	4.1.39
40.	stabl	4.1.40
41.	sst	4.1.41
42.	rutl	4.1.42
43.	srt	4.1.43

4.1.1

Title of the run: maximum 60 characters

4.1.2

Type of circuit considered: *driven* mode or *persistent* mode. Use *DRV* for this case

4.1.3

In this row two integers have to be inserted: the total number of coils (*ncoil*) and the number of power supplies (*necoil*)

4.1.4

This key can assume two integer values: 0 or 1. It allows choosing the model adopted for the calculation of the critical temperature $\Theta_c(B)$ and the critical generation temperature $\Theta_g(B,J)$ (see paragraph 3.3). *ncoil* values have to be inserted in the same row (one for each coil).

4.1.5

This is the co-sinus of the pitch angle of the strand of the Rutherford cable (see paragraph 3.5.3). *ncoil* values have to be inserted in the same row (one for each coil).

4.1.6

These three values represent the internal radius, the external radius and the total height of each coil. *ncoil* rows are expected, each one with three numbers.

4.1.7

timq is the time of the planned quench, *rquen* and *yquen* the radial and axial position of the center of the planned quench ellipsoid. *rquen* has to be between *rmin* and *rmax*, whereas *yquen* between 0 and *dh*. *Rrqui*, *hhqui* and *llqui* are the initial dimension of the semi-axis of the ellipsoid (in meters). *ncoil* rows are expected, each one with three numbers.

4.1.8

nzon is the number of the zones in radial direction in which the magnet is subdivided. *ncoil* rows are expected, each one with an integer number.

4.1.9

nzonh is the number of the zones in axial direction in which the magnet is subdivided. *ncoil* rows are expected, each one with an integer number.

4.1.10

R(ncoil,nzon) is the radial position on the voltage taps that subdivide the radial zones of each magnet. *ncoil* rows are expected, each one with an *nzon*+1 numbers.

4.1.11

d(ncoil,nzon) is the axial position on the voltage taps that subdivide the axial zones of each magnet. *ncoil* rows are expected, each one with an *nzonh*+1 numbers.

4.1.12

nh(ncoil,nzon,nzonh) is the grouping of consecutive radial zone for each axial zone. The voltages of the zones that have been grouped are summed in the output files and in the check of *vqds*. 1 means no grouping, 2 means grouping with the sequent radial zone, 3 means grouping with the 2 sequent radial zones, and so on. 0 means zone not considered because has been previously grouped. *nzonh* rows per *ncoil* are expected, each one with *nzon* integer numbers.

4.1.13

     ivel is a key that can assume value 1 or 2. It allows selecting which option use for the evaluation of the specific heat in the calculation of the velocity of propagation of quench (see paragraph 3.5.2). *theo* is the operation temperature of the magnet. *deltemp* is the maximum increment of temperature allowed for the resolution of the differential equation of the temperature (39) (see paragraph 3.8). One row is expected with three values.

4.1.14

     themax, *bmax* and *xlub* are the parameter necessary for the calculation of the critical temperature and critical generation temperature of each coil (see paragraph 3.3). *ncoil* rows are expected, each one with three numbers.

4.1.15

     These quantities are the values of the magnetic field in the cross section of the coils at the initial current (see paragraph 3.4). *ncoil* rows are expected, each one with seven numbers.

4.1.16

     num(Ic-B) is the number of couples current-field that in the following will be given in order to determinate the function critical current vs. field. *Alfa, beta* and *thecc* are other parameters to determinate this function (see paragraph 3.3). *num(Ic-B)* has to be greater than 1. *ncoil* rows are expected, each one with four numbers. WARNING: after each row, the corresponding rows of 4.1.17 have to be inserted.

4.1.17

     Ic and *B* are the couples of current-field to determinate the function critical current vs. field. *num(Ic-B)* rows are expected, after each row of paragraph 4.1.16. Each rows two number

4.1.18

     nc is the number of component of each coil. One row is expected, with *ncoil* values.

4.1.19

     mat is the name of the material, *frac* is the fraction in the unit cell, *rrr* is the resistivity residual ratio. *mattype* is a key: 1 means insulation material, 2 means metal, 3 means superconductor. *mat* is character string with 8 characters; capitalized character must be used. The main name used are 'COPPER ', 'ALUMINUM', 'NB3SN ', 'NBTI ', 'G10 ', 'BRONZE ', 'SN ', 'TANTALUM', 'SILVER ', . For each coil *nc* rows are expected (in total *ncoil* times *nc* rows). Each row four values.

4.1.20

   alr and *alh* are the radial dimension and the axial dimension of the unit cell. *Alinsr* and *alinsh* are the radial thickness and axial thickness of the insulation on each side of the unit cell

4.1.21

   vqds(ncoil,j,nzonh) is the resistive voltage that trigger the QDS for the opening the main circuit with the power supply. This voltage is between grouped voltage taps of radial zones. For each coil (*ncoil*), *nzonh* rows are expected (in total *ncoil* times *nzonh* rows). Each row contains a number of value equal to the number of grouped zones in that axial zone.

4.1.22

   hmuts(ncoil,nzon,nzonh,ncoil) is the mutual inductance of the each zone of each coil respect each coil. For each coil (*ncoil*) and for each radial zone (*nzon*), *nzonh* rows are expected (in total *ncoil* times *nzon* times *nzonh* rows), each one with *ncoil* numbers.

4.1.23

   amp0 and *rdump* are the initial current and the dumping resistor of each power supply. *ind* and *ivt* are parameters to select the function of the power supply (see paragraph 3.9.1.2). *necoil* rows are expected, each one with four numbers.

4.1.24

   timarc is time necessary to the extinguish the arc of the switch (see paragraph 3.9.1.4) and *deltime* is the total delay of the QDS (see paragraph 3.9.1.1). *necoil* rows are expected, each one with two numbers.

4.1.25

   nswi is a key for the opening of the switch of the power supply: if *nswi*=1 the switch of the power supply is opened as soon as a QDS detects a quench in any coil. If *nswi*≠1 the switch of the power supply is opened only if the QDS detects a quench in a coil of that power supply. A rows is expected, with *necoil* integers.

4.1.26

   This parameter control the working of the power supply (see paragraph 3.9.1.2). A rows is expected, with *necoil* numbers.

4.1.27

   This parameter control the working of the power supply (see paragraph 3.9.1.2). A rows is expected, with *necoil* numbers.

4.1.28

Parameter used for the power supply in case *ivt*=1 (see paragraph 3.9.1.2). A rows is expected, with *necoil* numbers.

4.1.29

This parameter defines, for each power supply, how many coils are connected in series. The sum of all *nacc* must be equal to *ncoil*. A rows is expected, with *necoil* numbers.

4.1.30

nts is the number of temporal steps of the run; *dt* is the temporal step; *iout* is a key: if *iout*=1 all the output files are printed. Otherwise the main output files only are printed (see paragraph 2). One row is expected, with three numbers.

4.1.31

Key for the choice of the thermal exchange between quenched coils and helium bath (see paragraph 3.11). An integer is expected.

4.1.32

These are coefficient for the thermal exchange between quenched coils and helium bath (see paragraph 3.11). One row is expected, with two numbers.

4.1.33

Total mass of the helium. One number is expected.

4.1.34

Coefficients for the correction of the velocities of propagation of the quench (see ends of paragraphs 3.1 and 3.2). *ncoil* rows are expected, each one with five numbers

4.1.35

Parameter used in the calculation of the quench velocities when there is a pre-heating of the conductor due to large heater (see paragraph 3.1.5). Normally is set equal to zero. *ncoil* rows are expected, each one with one number.

4.1.36

Key used to choose which model adopt for the calculation of quench velocities (see paragraph 3.1.1, 3.1.2, 3.1.3, 3.1.4). *ncoil* rows are expected, each one with one number.

4.1.37

Parameter used in the calculation of quench velocity when *kvl*=2. *ncoil* rows are expected, each one with one number.

4.1.38

Parameter used in the calculation of quench velocity when *kvl*=2. *ncoil* rows are expected, each one with one number.

4.1.39

Parameter used in the calculation of quench velocity when *kvl*=3. *ncoil* rows are expected, each one with one number.

4.1.40

Parameter used in the calculation of quench velocity when *kvl*=4. *ncoil* rows are expected, each one with one number.

4.1.41

Parameter used in the calculation of quench velocity when *kvl*=4. *ncoil* rows are expected, each one with one number.

4.1.42

Parameter used in the calculation of quench velocity when *kvl*=4. *ncoil* rows are expected, each one with one number.

4.1.43

Parameter used in the calculation of quench velocity when *kvl*=4. *ncoil* rows are expected, each one with one number.

4.2 Case in *persistent* mode (*PER*)

	Name of parameter	See paragr.
1.	Title of the run	4.1.1
2.	Type of circuit	4.2.1
3.	ncoil	4.2.2
4.	isc	4.1.4
5.	cosbeta	4.1.5
6.	rmin,rmax, dh	4.1.6
7.	timq, rquen, yquen, rrqui, hhqui, llqui	4.1.7
8.	nzon	4.1.8
9.	nzonh	4.1.9
10.	R(ncoil,nzon)	4.1.10
11.	d(ncoi,nzon)	4.1.11
12.	nh(ncoil, nzon, nzonh)	4.1.12
13.	ivel, the0, deltemp	4.1.13

14.	themax, bmax, xlub	4.1.14
15.	b0i,brinti,brexti,bhinti,bhexti,bexti	4.1.15
16.	num(Ic-B),alfa,beta,thecc	4.1.16
17.	Ic, B	4.1.17
18.	Nc	4.1.18
19.	mat,frac,rrr,mattype	4.1.19
20.	alr,alh,alinsr,alinsh	4.1.20
21.	rshunt	4.2.3
22.	vqds(ncoil,j,nzonh)	4.1.21
23.	hmuts(ncoil,nzon,nzonh,ncoil)	4.1.22
24.	amp0, rdump, ind, ivt	4.2.4
25.	timarc, deltime	4.2.5
26.	vmax1	4.2.6
27.	vmax2	4.2.7
28.	tau	4.2.8
30.	nts, dt, iout	4.1.30
31.	ienergy	4.1.31
32.	coetr, coeq	4.1.32
33.	elimass	4.1.33
34.	corvri,corvre,corvhu,corvhd,corvz	4.1.34
35.	tedi	4.1.35
36.	kvl	4.1.36
37.	acu	4.1.37
38.	adif	4.1.38
39.	difle	4.1.39
40.	stabl	4.1.40
41.	sst	4.1.41
42.	rutl	4.1.42
43.	srt	4.1.43

4.2.1

Type of circuit considered: *driven* mode or *persistent* mode. Use *PER* for this case

4.2.2

In this row an integers have to be inserted: the total number of coils (*ncoil*).

4.2.3

Values of the shunt resistors. A row is expected, with *ncoil* values.

4.2.4

    amp0 and *rdump* are the initial current and the dumping resistor of the power supply. *ind* and *ivt* are parameters to select the function of the power supply (see paragraph 3.9.1.2). One row is expected, with four numbers.

4.2.5

    timarc is the time necessary to the extinguish the arc of the switch (see paragraph 3.9.1.4) and *deltime* is the total delay of the QDS (see paragraph 3.9.1.1). One row is expected, with two numbers.

4.2.6

    This parameter control the working of the power supply (see paragraph 3.9.1.2). One row is expected, with one number.

4.2.7

    This parameter control the working of the power supply (see paragraph 3.9.1.2). One row is expected, with one number.

4.2.8

    Parameter used for the power supply in case *ivt*=1 (see paragraph 3.9.1.2). One row is expected, with one number.

5.   LIMIT OF THE PROGRAM

    In this section we want to collect the main limits of the code:

1. The origin of the quench is considered like a point that spreads in the following temporal step. This is an approximation, especially when large quench heaters induce the transition.
2. Numerical error can occur when large values for the dump resistor and shunt resistors are used. In fact the current equation are solved in single precision with a simple Eulero integration. The user has to reduce the values of dump resistors when this situation occurs.
3. Rough modeling of the magnetic field map, which influence the accuracy of resistance evaluation.
4. Coils are not thermally connected. So quench propagation among coils happens eventually through helium heating (it may be important for persistent magnet).
5. The dissipation for AC effect is not taken into account.

6.   CONCLUSION

    In this report we described the main features of the quench simulation code QLASA. The program allows calculating the hot spot temperature, the voltages, the current evolution, the energy distribution in multi-coil superconducting solenoids, with different configurations

for the electrical circuit (the coils can be power supplied in series, independently or without power supply in the persistent mode).

A particular care has been devoted in the exact calculation of the 3-D ellipsoid of the quenched volumes, in order to calculate the internal voltages if the coil is subdivided in more sections by voltage taps. Many models for the quench velocity calculation are foreseen in the code, which the user can select according to the different types of conductor.

The main limitation of the calculation is the hypothesis of complete adiabaticity inside the coil and among coils, i.e. heat diffusion is neglected. In any case this type of approximation normally results sufficient accurate for impregnated magnet and is moderately conservative in respect to the calculation of the hot spot temperature.

The program is conceived in such a way that some improvement may be relatively easy to be performed, as the implementation in the quench velocity calculation, better field map description and electrical circuit modification.

The code is linked to a custom cryogenic material property library (the subroutine XMATPRO), which deals with almost all materials used for classical superconducting magnet.

7.   REFERENCES

(1) M.N. Wilson, Superconducting Magnets, Claredon Press Oxford, (1983).

(2) S. Caspi, S. Bartlett, L. Chiesa, D.R. Dietderich, P. Ferracin, S. Gourlay, R. Hafalia, C. Hannaford, A. Lietzke, G. Sabbi, R. Scanlan, L. Imbasciati, Electro-thermo mechanical response to a quench in Nb3Sn magnets, IEEE Trans. on Applied Superconductivity, Vol. 14 N.2, (2004).

(3) E.M. Eyssa, W. Denis, Markiewicz, Charles A. Swenson, "Quench, thermal and magnetic analysis computer code for superconducnting magnets", IEEE Trans. on Mag., Vol. 32 N.4, p. 2659-2662, (1996).

(4) M. Canali, L. Rossi, Dynque: a computer code for quench simulation in adiabatic multicoil superconducting solenoids, INFN report, infn/tc-93/06, (1993).

(5) M. Sorbi, Studio della propagazione del quench e misure su avvolgimenti superconduttori adiabatici in NbTi e Nb3Sn, Graduation thesis, PACS code 85.25.S Milan University, Physics Department, (1994).

(6) M. Pellegatta Studies and measurements on the normal zone propagation following a quench in ATLAS/B0 superconducting magnet, Graduation thesis, PACS code 85.25.S Milan University, Physics Department, 19, (2002).

(7) W.H.Cherry, J.J.Gittleman, Solid state electronics, 1,287 (1960).

(8) L.Dresner, Proc. ASC 1978, IEEE Trans. on Mag., Mag-15 328 (1979).

(9) M.S. Lubell, Proc. ASC 1982, IEEE Trans. on Mag. Mag.-19, 754 (1983).

(10) L.T. Summers, M.W. Guinan, J.R. Miller, P.A. Hahn, A model for the prediction of Nb_3Sn critical current as a function of field, temperature, strain and radiation damage, IEEE Trans. on Mag., Vol.27-2, 2041, (1991).